AN ABSTRACT OF THE THESIS OF

Russell Everett Curtice for the Ph.D. in Inorganic Chemistry
(Name) (Degree) (Major)

Date thesis is presented November 14, 1963

Title The Luminescence of Thallium (I) Halide Complexes

Abstract approved Redacted for Privacy
(Major professor)

The fluorescence excitation and emission spectra of KCl:TlCl, KBr:TlBr, and KI:TlI solutions were measured in order to determine the spectral regions in which the thallous halide complexes fluoresce. For each type of solution, it was found that the fluorescence emission maximum is dependent on the composition of the solution and the wavelength of the excitation radiation. The excitation spectra were found to parallel the absorption spectra.

The nature and dissociation constants of yet unreported complex species were determined from the solubility data of Scott and Hu for KCl:TlCl solutions and from the solubility data of Kul'ba for KI:TlI solutions. Absorption measurements were made so that the molar absorptivities could be determined for each of the complex species. Evidence is given that in KCl solutions of concentration greater than 2.5 M a complex ion of formula $TlCl_4^{=}$ (dissociation constant, 93; absorption maximum, 253 mμ) exists. Dissociation constants were also determined for TlI, TlI_2^{-}, $TlI_3^{=}$, and $TlI_4^{\equiv}$ complex species; however, the molar absorptivities of these complexes were not obtained.

The fluorescence emission spectra of KCl:TlCl and KBr:TlBr solutions were analyzed with the assistance of the dissociation constants of the complex species. The broad fluorescence band of the chloride solutions with maximum at 440 mμ was determined to be due to the overlap of four symmetric bands, which have a maximum of 370, 435-440, and 450 mμ for Tl^+, TlCl and $TlCl_2^-$, and $TlCl_4^{\equiv}$ respectively. For KBr:TlBr solutions, the broad fluorescence band with maximum at 480 mμ is due to the overlap of three bands with a maximum at 440 mμ for TlBr, 475 mμ for $TlBr_2^-$, and 495 mμ for $TlBr_4^{\equiv}$. The order of the fluorescence quantum yield is $TlCl_4^{\equiv} > TlCl_2^- \cong TlCl > Tl^+$ and $TlBr > TlBr_2^- > TlBr_4^{\equiv}$.

The fluorescence intensity of KI:TlI solutions, in contrast to the strong fluorescence of thallous chloride and thallous bromide complexes, is very weak. This weak fluorescence intensity may be due to dissipation of the energy by photochemical reactions or quenching by iodide ions.

The dissociation constants of TlX complexes were used to calculate thallium-halide single bond energies by a thermochemical cyclic process.

The absorption spectrum of thallous halide complexes was considered from the standpoint of electron transfer transitions. The absorption maximum of these transitions is shifted toward longer wavelengths as the reducing strength increases and as the number of coordinated halide ligands increases. The oscillator strengths of the transitions are approximately 0.1. It is postulated that an

electron is transferred from a halide ligand to the thallous ion.

The similarity of the absorption and emission spectra of thallium-containing potassium halide single crystal phosphors with that of the thallous halide complexes is demonstrated; the conclusion is made that the spectra of the single crystal phosphors may be attributed to complex aggregates in the crystal lattice and that treatment of the spectra from the standpoint of electron transfer would be worthwhile.

THE LUMINESCENCE OF THALLIUM (I) HALIDE COMPLEXES

by

RUSSELL EVERETT CURTICE

A THESIS

submitted to

OREGON STATE UNIVERSITY

in partial fulfillment of
the requirements for the
degree of

DOCTOR OF PHILOSOPHY

June 1964

APPROVED:

Redacted for Privacy

Professor of Department of Chemistry

In Charge of Major

Redacted for Privacy

Chairman of Department of Chemistry

Redacted for Privacy

Dean of Graduate School

Date thesis is presented November 14, 1963

Typed by Penny A. Self

ACKNOWLEDGMENTS

The author would like to express his sincere appreciation to Dr. Allen B. Scott for having suggested this investigation and for his assistance, suggestions, and comments in the preparation of this thesis.

The author wishes to thank Dr. Virgil Freed for the use of the Aminco-Bowman spectrophotofluorometer and Dr. Clara Storvick and staff not only for the use of the aforementioned instrument but also for their generosity and encouragement.

The author would also like to express his gratitude to Mrs. Penny Self for the preparation of the manuscripts and to Mr. David MacEachern for the drafting work.

TABLE OF CONTENTS

TABLE OF CONTENTS Continued

LIST OF FIGURES

LIST OF FIGURES Continued

LIST OF TABLES

LIST OF TABLES Continued

THE LUMINESCENCE OF THALLIUM (I) HALIDE COMPLEXES

I. INTRODUCTION

In the period 1929 - 1933, many investigators observed that if TlCl is added to aqueous solutions of KCl or to KCl melt, then new absorption and emission bands, which are not characteristic of KCl itself, are observed. Because of the similarity of the absorption and emission spectrum of KCl:Tl single crystal phosphors with that of KCl:TlCl solutions, the same mechanism likely is responsible for the observed spectra. There is, however, no agreement as to the mechanism responsible for the luminescence properties of each.

The present investigation was undertaken, therefore, to study in detail the luminescence of potassium halide solutions containing the corresponding thallous halide. It is hoped that this investigation and the proposals therein will help elucidate the structure and mechanism responsible for the luminescence of single crystal KCl:Tl phosphors.

Before reviewing the investigations which have been made on single crystal thallium-activated potassium halide phosphors and on thallous halide-alkali halide solutions, the luminescence process will be treated briefly.

A. Review of the Luminescence Process

Luminescence is a general term applied to light emission excited by energy absorption. Luminescence is categorized by the type of energy that is absorbed. Thus such terms as photoluminescence, thermoluminescence, chemiluminescence, and others describe the form of energy being absorbed. Photoluminescence is further classified into phosphorescence and fluorescence. Although there is no general agreement as to the distinction between fluorescence and phosphorescence, the usual distinction between the two is based upon the lifetime of the excited state; the excited state for fluorescence has the shorter lifetime. The lifetime of the excited state is also used as a criterion for distinguishing luminescence phenomena from other emission processes, such as the Raman effect, Rayleigh scattering, and Cherenkov radiation.

According to Bohr's theory of discrete energy levels, when a quantum of energy is absorbed by a molecule, atom, or ion, an electron may be excited from a lower energy level to a higher energy level by absorbing a quantum of energy which is equal to the difference between the energies of these two quantum states. The quantum of energy is absorbed in approximately 10^{-15} seconds, which is so rapid that the internuclear distances may be considered as remaining constant during the absorption process.

In the case of luminescence, the now excited electron state persists for a finite time, 10^{-8} seconds, whereas the Raman effect

and Rayleigh scattering are completed in 10^{-14} seconds or less. According to Pringsheim (47) and other authors the lifetime of the excited state in the case of fluorescence is approximately 10^{-8} seconds, whereas for phosphorescence the lifetime is longer.

The process of photoluminescence for the thallous ion may be envisaged as follows: (1) The molecule selectively absorbs a photon of light and is raised to one of the many vibrational levels of the first excited singlet state. (2) Due to collisions and partition of this energy to other electronic, rotational and vibrational modes, the molecule rapidly loses energy and drops to the lowest vibrational level of the first excited state. (3) The molecule then returns to the ground state emitting fluorescent radiation at higher wavelength (lower energy) than that of the absorbed radiation. If a second series of excited states, the triplet states, having energy values close to that of the excited singlet state, are also present in the molecule, the molecule may shift from the singlet excited state to the triplet. Since direct transitions from singlet to triplet states are "forbidden" by the selection rules, the electron can return to the ground state only after a measurable time delay by means of the forbidden transition or via the singlet excited state. This time-delayed, temperature-dependent emission is termed phosphorescence.

The lifetime of an excited state is measured by following the luminescence decay which obeys an exponential decay law of the form $I_t = I_o e^{t/\tau}$, where I_t is the fluorescence intensity at time t, t is the time since removing the excitation source, I_o is the intensity of

fluorescence at t = 0, and τ is the average lifetime of the excited state.

The concentration dependence of luminescence may be derived from a consideration of the Beer-Bouguer-Lambert law. If the Beer-Bouguer-Lambert law is assumed to be applicable to the radiation absorbed by the sample, then by defining a new proportionality constant, ϕ, the fluorescence flux is given by the expression

$$F = I_o (1 - e^{-\epsilon cx}) \phi \quad ,$$

where F is the total fluorescent flux in quanta per second, I_o is the flux of the excitation radiation in quanta per second, ϵ is the molar absorptivity, x is the thickness of the sample, c the concentration of the fluorophor or luminophor, and ϕ the quantum yield of the process. The quantum yield, ϕ, is defined as the ratio of the number of quanta emitted to the number of quanta absorbed. This quantitative relationship between fluorescence flux and concentration has been proven by measurements on rhodamine and uranin solutions (47).

At low concentration values, the above relationship between F and c becomes:

$$F = (I_o \epsilon cx\phi) \quad .$$

(Bowen and Stokes (62) showed that this linear dependence of F on c is only applicable to solutions in which less than 5% of the exciting radiation is absorbed.) At high concentrations, the equation

approaches the limit:

$$\underset{C\to\infty}{F} = \phi I_o$$

Thus, for those solutions in which all of the light is absorbed by the layer under consideration, the fluorescence flux should approach the limit ϕI_o. In reality this limit is seldom realized; instead the fluorescent intensity reaches a maximum at some "optimum concentration" and then decreases with increasing concentration of luminophor. This apparent decrease in fluorescence intensity would seem to indicate that the quantum yield is a function of concentration. A further consideration is that since F is proportional to I_o, then in highly concentrated solutions the first layer of solution will absorb part of the radiation and each subsequent layer will have less radiant energy available for excitation thus the first layer will have the greatest fluorescence flux. This apparent decrease of fluorescence is sometimes referred to as "concentration quenching" or loss due to an inner filter effect.

B. Review of Single Crystal Phosphors of Thallium Activated Alkali Halides

The incorporation of a small amount of a thallium halide in the corresponding alkali halide crystal lattice is accompanied by new absorption bands in that region of the spectrum where the alkali halide is transparent. When excited by ultraviolet radiation, these thallium-activated alkali halide phosphors exhibit phosphorescence

and fluorescence.

In 1931, Buenger and Flechsig (9) quantitatively investigated the luminescence properties of thallium-activated potassium chloride phosphors. They found that pure potassium chloride has absorption maxima at 163 and 200 $m\mu$; however, upon the introduction of thallous chloride, new absorption bands with maxima at 196 and 247.5 $m\mu$ were observed. The luminescence is comprised of a short lived fluorescence and a prolonged phosphorescence. The fluorescence and phosphorescence emission spectra are identical and consist of two wide bands with maxima at 310 and 470 $m\mu$. They also indicate that absorption at 247.5 $m\mu$ gives rise only to fluorescence while absorption at 196 $m\mu$ gives rise to both fluorescence and phosphorescence.

Other thallium activated potassium halide phosphors have been investigated. The potassium bromide: thallium phosphors (47) have absorption maxima at 210 and 262 $m\mu$, and emission maxima at 318 $m\mu$ and 430-500 $m\mu$. The potassium iodide: thallium phosphors (69) have absorption maxima at 236 and 287 $m\mu$, and a broad emission band with maximum at 440 $m\mu$.

Many other studies have been made on these phosphors in order to determine the temperature dependence (3, 31), the quantum yield (42), the kinetics (63), quenching (12), polarization (39), and other facets of the luminescence of these phosphors.

The mechanism responsible for the absorption and emission of these phosphors has received much theoretical consideration.

Seitz (57), in 1938, assumed that the thallium (I) ion occupies the site of a potassium (I) ion in the host lattice and that the absorption as well as the emission spectra could be interpreted on the basis of electronic transitions occurring within the thallium (I) ion. Using Seitz's model, Williams and coworkers (26-29, 66-68) have developed a theory for the luminescence center. They abscribe the main absorption and emission bands to transitions between the ^1S_o ground state, $6s^2$ configuration, and the perturbed $^3P_1$ and $^1P_1$ state with 6s6p configuration. The energies of the ^1S_o, $^3P_1$, and $^1P_1$ states were calculated by quantum mechanics. The absorption and emission spectra were determined from configurational coordinate diagrams and these spectra agree quite satisfactorily with the observed spectra.

The Seitz-Williams model for the luminescence center, while widely accepted, leaves unanswered many details of the luminescence properties of these phosphors. Some of the objections that have been made are:

(1) X-ray studies of these phosphors show that on the addition of thallous ion, the potassium chloride crystal lattice is stretched by a much smaller amount than would be expected if the thallous ion (ionic radius, 1.51 Å) replaces the potassium ion (ionic radius, 1.33 Å). The conclusion is made that the phosphors should be considered as mixed crystals rather than as single crystals (54).

(2) The model does not explain the origin of trapping states which dominate the phosphorescence; nor does it identify the impurity system and electronic states responsible for longer wavelength emission bands (67).

Other authors have used different models to explain the luminescence of the solid phosphors. Due to the similarity of the absorption and emission spectra of alkali halide solutions containing a thallous halide with that of the corresponding phosphors, Pringsheim (49) and Hilsch (23) suggested that luminescence properties of the solutions and crystal phosphors should be attributed to thallous halide complex ions. Ivanova and coworkers (25) concluded that the different luminescence bands of a phosphor must be attributed to different centers and that these centers are of the molecular complex type, involving both the base material and the activator. In those phosphors involving transition group metals, a ligand field or crystal field approach to the splitting of the d levels in a complex has been successful in interpreting the luminescent spectra.

C. Review of the Thallous Halide-Alkali Halide Solutions

In contrast to the numerous investigations that have been carried out on thallium-activated alkali halide crystal phosphors, the aqueous solutions of alkali halides containing small amounts of the thallous halide have received much less experimental and theoretical consideration. Fromherz and Menschick (16) in 1929, Hilsch (23) in 1937, and Pringsheim (49) in 1940 indicated that the

luminescence properties of such solutions could be ascribed to complex ions of the type TIX_n^{1-n} . Fromherz (15) concluded that the formation of phosphorescent centers in crystals and the formation of complex ions in solution are produced by chemically similar processes. As evidence, may be cited the close similarities in the absorption spectra as shown in Figure 1 (47).

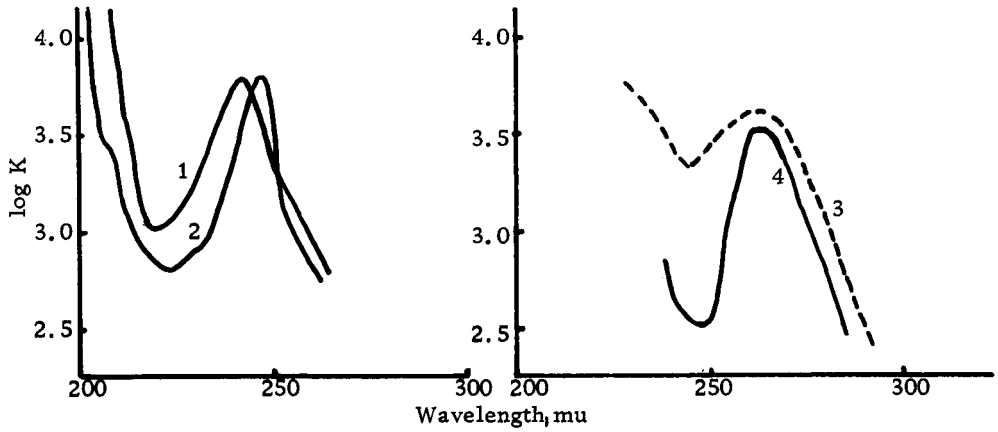

Figure 1. Absorption bands of Tl in alkali halide phosphors and aqueous alkali halide solutions

1) KCl:TlCl solution
2) KCl:Tl phosphor
3) KBr:TlBr solutions
4) KBr:Tl phosphor

Pringsheim and Vogels (49) reported that the KCl:TlCl solutions have fairly strong blue fluorescence (maximum at 435 $m\mu$) arising from excitation at 247 $m\mu$ and the KBr:TlBr solutions emit a blue green fluorescence (maximum at 460 $m\mu$) arising from excitation at 265 $m\mu$. A much weaker ultraviolet emission band was also reported for these solutions. Pringsheim (48) also found that if the solution is supersaturated so that salt begins to crystallize

out, the solution loses its ability to fluoresce and the selective bands in the absorption spectrum disappear. If the precipitated crystals are then redissolved in a potassium halide solution, a measure of the fluorescence of the solution proved that 99% of the original thallium was in the crystals. The precipitated crystals obtained are strongly fluorescent and phosphorescent and have selective absorption bands with maxima at 195 and 247.5 $m\mu$ for the chloride and at 200 and 261 $m\mu$ for the bromides. In contrast to the crystal phosphors, the visible fluorescence is very strong for solutions and precipitated crystals.

The most recent investigations have been those due to Avramenko and Belyi (2), Shinoya (58) and coworkers, and Brauer and Pelte (7). Avramenko and Belyi investigated the luminescence spectra of KCl:TlCl and KBr:TlBr solutions. They attribute the 430 $m\mu$ emission of the chloride solutions to TlCl and $TlCl_4^{\equiv}$ and the 470 $m\mu$ emission of the bromide solutions to TlBr, $TlBr_3^{=}$, and possibly $TlBr_4^{\equiv}$. They also report that the spectra are altered relatively little by a change in temperature.

Brauer and Pelte have also studied the luminescence of KCl: TlCl and KBr:TlBr solutions. In contrast to the conclusion of Avramenko and Belyi, Brauer and Pelte concluded that the broad luminescence band of the chloride solutions is due to the overlap of three symmetric bands. The three bands are due to Tl^+, TlCl, and $TlCl_2^-$ with maxima at 368 $m\mu$, 395 $m\mu$, and 440 $m\mu$ and half-widths of 5300 cm^{-1}, 4950 cm^{-1}, and 4750 cm^{-1} respectively.

Analogous results seem to apply to KBr:TlBr solutions; however, they did not assign a definite band to a definite complex for the bromide solutions.

Meritt and coworkers (41) and Sill (60) have studied the absorption and fluorescence of thallium (I) chloride complexes as an analytical method for the detection of thallium.

Evidence that complex ions of the type TlX_n^{1-n} exist in solution is manifold. Scott and Hu (24, 55), Nilsson (44), and Kul'ba and coworkers (36-38) have studied complex ion formation using solubility studies, absorption studies, and potentiometric titrations. Scott and Hu have determined the dissociation constants and molar absorbtivities for TlCl and $TlCl_2^-$ and indicate that higher complexes of undetermined nature are also probably present. For KBr:TlBr solutions Scott, Dartau and Sapsoonthorn (56) have reported the dissociation constants and molar absorptivities for TlBr, $TlBr_2^-$, and $TlBr_4^{---}$ complexes. Kul'ba and coworkers indicate that in KI:TlI solutions complexes of the type TlI, TlI_2^-, TlI_3^{--} and TlI_4^{---} probably exist.

D. Objectives

The objectives of this investigation are:

(1) to measure quantitatively the luminescence spectra of KCl:TlCl, KBr:TlBr, and KI:TlI solutions.

(2) to determine the spectral region in which the various complex species of thallium luminesce.

(3) to determine the nature of complexes not yet reported.

(4) to correlate the observed absorption and emission data with theoretical calculations based on the geometry and bonding in the complex.

II. EXPERIMENTAL PROCEDURE

A. Stock Solutions

In all instances the reagents were doubly recrystallized from distilled water, washed with 100% ethanol, and dried at 100°C for 24 hours. The stock solutions were made by weighing the recrystallized salt to an accuracy of 0.1 mg and then dissolving in the requisite amount of distilled water in volumetric flasks. Thus all solutions were made on the basis of volume concentration.

In Table 1 are listed the molar concentrations of potassium halide and thallous halide in each of the aqueous solutions studied.

B. Absorption Studies

Since extensive absorption studies have been made on the chloride (55) and bromide (56) solutions, the only extensive absorption measurements were those on the 3.0 and 4.0 molar KCl:TlCl solutions and KI:TlI solutions. The purposes of making these absorption measurements were (1) to determine if there are similarities between the absorption and excitation spectra, (2) to ascertain in conjunction with solubility studies, the formulas, dissociation constants, and molar absorptivities of yet undetermined thallous complexes, and (3) to determine whether the luminescence is absorbed by the solutions.

The absorption spectra were measured by means of a Beckman Model DU or Beckman Model DK-1 spectrophotometer.

Table 1. Concentration of aqueous solutions

Series	Potassium halide conc., mole/liter	Thallium concentration x 10^5, mole/liter
I. Chloride		
a)	0.0	a) 0.83, 1.66, 3.33, 6.67, 13.3, 26.6, 53.3, 80.0, 106, 133, 160, 186, 213, 240
b)	0.25 0.50 1.00 1.50 2.00	b) 0.0, 0.83, 1.66, 3.33, 6.67, 13.3, 26.6, 53.3, 80.0, 106, 133, 160
c)	3.0	c) 0.0, 0.83, 1.66, 3.33, 6.67, 13.3, 26.6, 53.3, 80.0, 106, 133, 160, 186
d)	4.0	d) 0.0, 0.83, 1.66, 3.33, 6.67, 13.3, 26.6, 53.3, 80.0, 106, 133, 160, 186, 213, 240
II. Bromide		
a)	0.0	a) 0.066, 0.13, 0.26, 0.53, 1.07, 2.67, 5.34, 10.7, 21.3
b)	0.50 1.0	b) 0.0, 0.066, 0.13, 0.26, 0.53, 1.07, 2.67, 5.34
c)	2.0	c) 0.0, 0.066, 0.13, 0.26, 0.53, 1.07, 2.67, 5.34, 10.7
d)	3.0 4.0	d) 0.0, 0.066, 0.13, 0.26, 0.53, 1.07, 2.67, 5.34, 10.7, 21.3
III. Iodide		
a)	0.0	a) 0.0067, 0.013, 0.026, 0.053, 0.107, 0.537, 1.07, 2.68, 8.06
b)	0.5 1.0	b) 0.0, 0.0067, 0.013, 0.026, 0.053, 0.107, 0.268, 1.07
c)	2.0	c) 0.0, 0.0067, 0.013, 0.026, 0.053, 0.107, 0.537, 1.07, 2.68, 5.37, 8.06
d)	3.0 4.0	d) 0.0, 0.0067, 0.013, 0.026, 0.053, 0.107, 0.537, 1.07, 2.68, 5.37, 8.06, 10.7
e)	5.0	e) 2.68, 5.37, 8.06, 10.7

A hydrogen lamp was used as the source for measurements in the region from 220 mμ to 340 mμ and a tungsten lamp in the region from 400 mμ to 520 mμ. Matching cells were used with distilled water as the reference standard.

C. Luminescence Measurements

The excitation and emission spectra of each solution were measured by means of an Aminco-Bowman spectrophotofluorometer. These measurements were at first made using the model equipped with a Hanovia Xenon arc and A.C. ballast; however greater stability of the xenon arc was obtained with the model equipped with a Osram 150 W xenon arc and a D.C. power supply.

A schematic diagram of the Aminco-Bowman spectrophotofluorometer is shown in Figure 2. The radiation from the xenon arc, after being dispersed by a Czerny-Turner type monochromator, is focused on the center of the cell compartment. The emitted radiation, which is detected at an angle of 90 degrees to the path of the exciting radiation, is similarly dispersed and focused on a slit in front of the photomultiplier tube. Seven slits may be used (three for the exciting radiation, three for the emitted radiation, and one in front of the photomultiplier tube). Various slit width arrangements were tried and the arrangement that resulted in optimum performance was selected. The cell used for the solution is made of fused quartz, has four optical surfaces, and external dimensions of 12 x 12 x 48 mm (10.5 x 10.5 mm internal diameter). An RCA

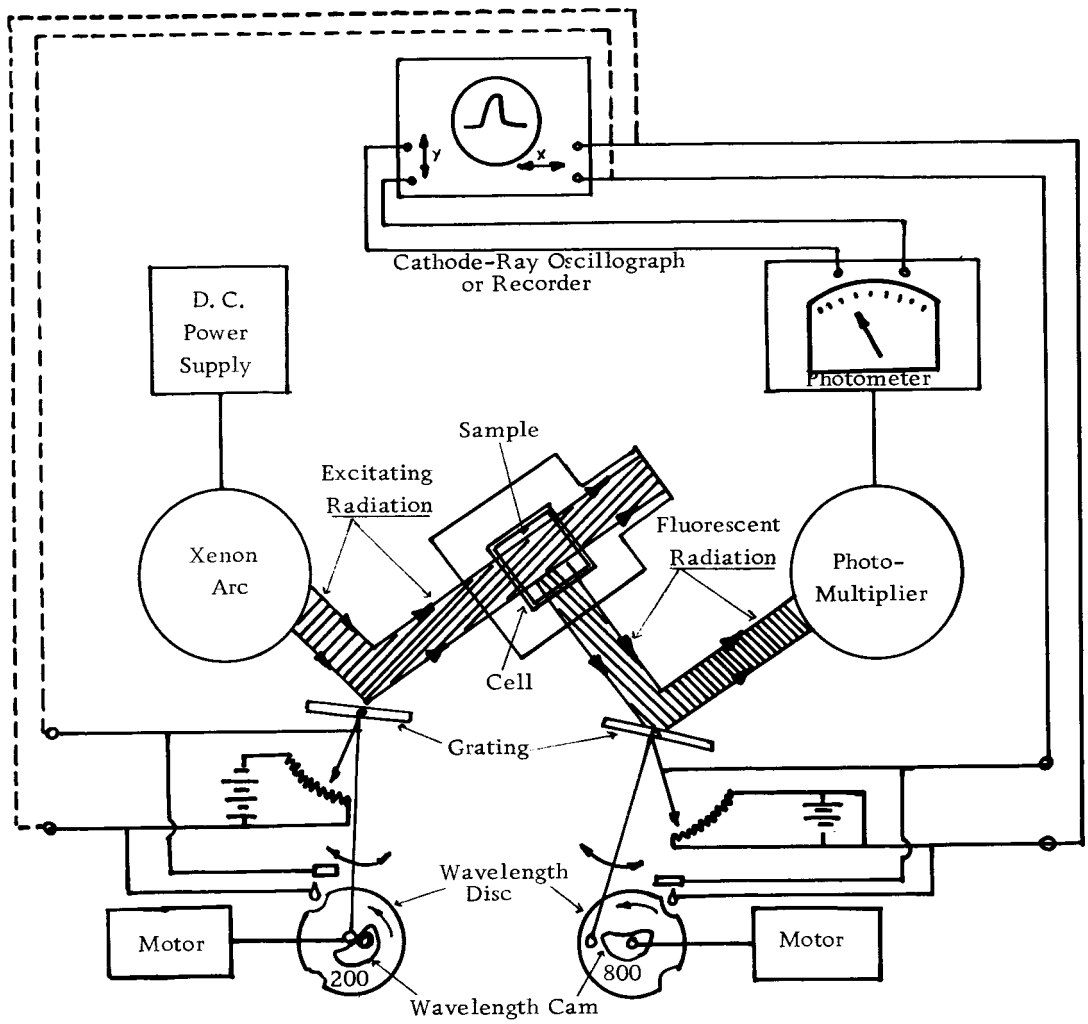

Figure 2. Schematic Diagram of Aminco-Bowman Spectrophotofluorometer

type 1P28 photomultiplier tube was used.

The excitation spectra were obtained by maintaining the emission monochromator at some fixed setting, usually an apparent fluorescence maximum, and then recording the fluorescence emitted as a function of the excitation wavelength. The emission spectra are records of the fluorescence emitted at a fixed excitation wavelength. These spectra may be recorded either by direct reading of the photomultiplier photometer as was done for the chloride solutions or by using an Electro Instruments Company 101 x-y recorder as was done for the bromide and iodide solutions.

D. Calibration of the Excitation and Emission Monochromators

The emission monochromator was calibrated using a "Pen-Ray" quartz lamp. The "Pen-Ray" quartz lamp provides an intense source of mercury lines. The fluorescence spectrophotometer was turned on and the lamp inserted in the cell compartment. Using the principal (and second order) lines of mercury, a peak photometer response should be found when the wavelength reading on the emission monochromator corresponds to one of the mercury lines. In those instances where such a correspondence was not obtained, the cam was adjusted.

The excitation monochromator was then calibrated against the emission monochromator which had been calibrated by the above method. This was done by turning on the xenon arc and placing glycogen, a highly scattering material, in the cell in the cell

compartment. When the two monochromators are properly aligned, a maximum photometer response should occur when the wavelength readings on the two monochromator cams coincide. If this coincidence was not found, then the excitation wavelength cam was adjusted.

E. Calibration of the Spectrophotofluorometer

The excitation and emission spectra obtained directly from the spectrophotofluorometer are to be regarded as uncorrected. In order to obtain true or corrected spectra, it was necessary to measure the quantum output of the xenon arc as a function of wavelength and to correct for the spectral response of the photomultiplier tube.

The quantum output of the xenon arc was found using the method of Parker and Hatchard (21) as modified by White (65). Potassium oxalato ferrate (III) was prepared by adding 900 ml of 1.5 M $K_2C_2O_4$ to 300 ml of 1.5 M $FeCl_3$. The mixture was cooled to 0°C to crystallize the green complex salt. After three recrystallizations in warm water, the salt was dried in a current of air at 45°C. The 0.006 M actinometer solution was made by dissolving 2.947 g of the complex salt, $K_3Fe(C_2O_4)_3 \cdot 3H_2O$, in 800 ml of water, adding 100 ml of the 1.0 N H_2SO_4, diluting to one liter, and mixing. The solution was stored in an amber bottle in the dark room.

The actinometry was carried out in the dark except for two darkroom safety lamps. Three-milliliter samples of the 0.006 M actinometer solution were pipetted into two one-centimeter silica

cells. One cell was placed in a dark box and was used as the blank. The other cell was placed in the cell compartment of the spectrofluorometer and irradiated for 15 minutes. The three slits between the cell compartment and xenon arc monochromator had slit widths of 1/8 inch, 1/16 inch and 1/8 inch respectively.

After the 15 minute irradiation time had elapsed, one ml aliquots were drawn from each cell and placed in 25 ml volumetric flasks. To each flask was added 11.5 ml of 0.1 N H_2SO_4, 2.5 ml of 0.1% o-phenanthroline monohydrate, 6.4 ml of sodium acetate-sulfuric acid buffer, and water to the 25 ml mark. These samples were allowed to stand in the dark for one-half hour. The absorbance of each sample was measured at 510 mμ (one cm cell, Beckman DU). After subtracting the blank value, the difference in optical density was converted to moles of ferrous iron per ml using a calibration curve. Finally, the quantity of ferrous iron in the three ml irradiated sample was converted to radiation dose using the quantum efficiencies recommended by Parker (21).

The calibration curve for ferrous ion was made by adding to a series of 25 ml volumetric flasks, 0, 0.5, 1.0, 2.0, 2.5, ... 10 ml of 0.41×10^{-6} moles/ml of Fe^{++} in 0.1 N H_2SO_4. The ferrous ion solution was freshly prepared by diluting standardized 0.0822 M $FeSO_4$ (in 0.1 N H_2SO_4). Sufficient 0.1 N sulfuric acid was added so as to make the total acidity equivalent to 12.5 ml of 0.1 N sulfuric acid. Two and one half ml of 0.1% o-phenanthroline, 6.4 ml of sodium acetate-sulfuric acid buffer, and water to the 25 ml mark

were also added. The solutions were allowed to stand in the dark for at least 30 minutes; after which time the optical density of each solution was measured at 510 mμ. Each optical density was corrected by subtracting the optical density of the solution to which no ferrous ion had been added. The resulting difference optical density was plotted against the moles per ml of ferrous ion added. A linear calibration curve was obtained.

In order to measure the flux of the fluorescence radiation, two calibration methods were tried. The first method was the use of a thermopile-galvanometer system positioned at the entrance slit to the photomultiplier housing of the Aminco-Bowman spectrophotofluorometer. Since the fluorescence radiation, after being made monochromatic, was too weak to be detected by the thermopile-galvanometer system, a photographic method was used for the calibration.

The film, which had been placed in a lensless 36 mm Leica camera, was calibrated by exposure to a carbon filament lamp calibrated by the National Bureau of Standards. The exposure time varied from one to ten seconds and lamp-to-camera distances of two, three, four, five, and six meters were used. The film was also exposed to the fluorescence radiation from KCl:TlCl and KBr:TlBr solutions. After developement of the film, the optical density of the silver deposit was read on a Photovolt densitometer. Three film types, Kodak Panatomic-X, Kodak Plus-X, and Kodak Tri-X, were used and the film that gave the best correspondence between the optical density of silver deposit and the radiant energy striking it

was used.

F. pH measurements

Since the fluorescence intensity and wavelength of many substances is strongly pH dependent, the pH of the KCl:TlCl and KBr:TlBr solutions were measured. A Beckman Laboratory Model G pH Meter, which had been calibrated against known standards, was used for these measurements.

G. Effect of substitution of KNO_3 for KCl in the thallium-containing solid

In order to ascertain the effect of substituting KNO_3 for KCl in a KCl:Tl crystal phosphor, KNO_3 (m.p. 334°C) was melted in a muffle furnace. To the KNO_3 melt was added recrystallized TlCl. No attempt was made to grow single crystals. Thin sections and fine powders of the solid sample were placed in the cell compartment of the spectrophotofluorometer in order to determine if the thallium-containing KNO_3 sample is fluorescent.

III. EXPERIMENTAL RESULTS AND CALCULATIONS

A. Absorption measurements

KCl:TlCl solutions were found to fluoresce in the blue region of the spectrum with a band maximum at 430 mμ. The fluorescence of KBr:TlBr is emitted in the blue-green with a band maximum at 470 mμ. Absorption studies were made on KBr:TlBr and KCl:TlCl solutions in order to determine whether the emitted radiation was absorbed internally. In the wavelength range from 350 to 550 mμ, it was found that for both types of solutions the absorbance was negligible.

1. KCl:TlCl solutions. Since the solubility (24) and absorption (55) data for KCl:TlCl solutions indicate the probable presence of complexes of coordination number greater than two at chloride concentrations greater than 2.5 M, the optical density of 3.0 M and 4.0 M solutions were measured. This data in conjunction with Hu and Scott's data was used to determine formulas, dissociation constants, and molar absorptivities for the assumed complexes.

The method used for determining the formulas and dissociation constants of the complexes was essentially that due to Hu and Scott. The solubility data was treated graphically by plotting (solubility-$[Tl^+]$) versus $[Cl^-]$, where brackets indicate concentrations. The plot was linear at low chloride ion concentrations; however, at chloride concentrations greater than 2.5 M, there was a definite upward curvature. For that portion of the plot that is linear, the

least squares criterion was used to determine the slope and intercept, from which the dissociation constants of $TlCl_2^-$ and TlCl were determined. The following equilibria and dissociations constants were consistent with the data:

$$TlCl = Tl^+ + Cl^- \qquad K_1 = \frac{[Tl^+][Cl^-]\, f_\pm^2}{[TlCl]} = 0.25$$

$$TlCl_2^- = TlCl + Cl^- \qquad K_2 = \frac{[TlCl][Cl^-]}{[TlCl_2^-]} = 1.87$$

where $f_\pm$ is the mean activity coefficient for KCl. Since the concentration of a singly charged ion enters in both numerator and denominator of K_2 it is, to a first approximation, a thermodynamically correct constant, as is K_1.

For KCl concentrations greater than 2.5 M, the solubility in excess of that due to Tl^+, TlCl, and $TlCl_2^-$ was calculated. Complexes of the type $TlCl_3^=$, $TlCl_4^{\equiv}$, $TlCl_5^{-4}$, and $TlCl_6^{-5}$ were assumed to exist. The excess solubility, Δ, at a given chloride ion concentration, assuming for example $TlCl_3^=$ and $TlCl_4^{\equiv}$ complexes, is given by

$$\Delta = \frac{[TlCl_2^-][Cl^-]}{K_{3_c}} + \frac{[TlCl_2^-][Cl^-]^2}{K_{4_c}} ,$$

where $K_{3_c} = \dfrac{[TlCl_2^-][Cl^-]}{[TlCl_3^=]}$ for the equilibrium

$$TlCl_3^= = TlCl_2^- + Cl^-$$

and $K_{4_c} = \frac{[TlCl_2^-][Cl^-]^2}{[TlCl_4^{\equiv}]}$ for the equilibrium

$$TlCl_4^{\equiv} = TlCl_2^- + 2\,Cl^- .$$

By choosing different chloride ion concentrations, several such equations were obtained. The equations were solved simultaneously in order to obtain the dissociation constants for the assumed complexes. This process was repeated for other combinations of assumed complexes. The result most consistent with the data was that:

1) A $TlCl_4^{\equiv}$ complex probably exists at chloride concentrations greater than 2.5 M. The dissociation constant for the equilibrium

$$TlCl_4^{\equiv} = TlCl_2^- + 2\,Cl^-$$

is given by the expression

$$K_{4_c} = \frac{[TlCl_2^-][Cl^-]^2}{[TlCl_4^{\equiv}]} = 93.$$

2) At chloride concentrations greater than 3.2 M, a $TlCl_6^{-5}$ complex probably exists. The equilibrium and dissociation constant are given by:

$$TlCl_6^{-5} = TlCl_2^- + 4\,Cl^-$$

$$K_{6_c} = \frac{[TlCl_2^-][Cl^-]^4}{[TlCl_6^{-5}]} = 1800.$$

Since K_{4_c} and K_{6_c} are constants involving concentrations rather than activities, their validity is limited to the chloride ion concentration given for each.

The above determined values of the dissociation constants were used to determine the molar absorptivities of the complex species. The absorption spectra of 0.969, 1.88, 2.74, 3.0, and 4.0 M KCl solutions containing TlCl were analyzed according to the method of Hu and Scott. Letting t, u, v, w, x, and z represent the concentration, in mole/liter, of total Tl(I), Tl^+, TlCl, $TlCl_2^-$, $TlCl_4^{=}$, and Cl^- respectively, then the absorbance per cm A/b, is given by

$$A/b = u\epsilon_u + v\epsilon_v + w\epsilon_w + x\epsilon_x + z\epsilon_z$$

where ϵ is the molar absorptivity of the species denoted by the subscript. This equation, when combined with the dissociation constants defined on pages 23 and 24, gives

$$\frac{A}{b} - z\epsilon_z = A' = w\left[\frac{z^2}{K_{4_c}}\epsilon_x + \epsilon_w + \frac{K_1K_2}{z^2 f_\pm^2}\epsilon_u + \frac{K_2}{z}\epsilon_v\right].$$

The net absorbance per cm, A', was plotted against w at z = 0.96, 1.88, 2.74, 3.0 and 4.0 M for wavelengths of 240, 245, 250, 255, 260, 265, and 270 mμ. Corresponding to each value of z is a slope equal to

$$\text{Slope} = \frac{z^2}{K_{4_c}}\epsilon_x + \epsilon_w + \frac{K_1K_2}{z^2 f_\pm^2}\epsilon_u + \frac{K_2}{z}\epsilon_v .$$

These linear equations were solved simultaneously to obtain the value of ϵ for each species; however the value of ϵ_u and ϵ_y, previously determined by Hu and Scott, were used. The analysis substantiated the assumption that the $TlCl_4^{=}$ complex was present; however, the existence of the $TlCl_6^{-5}$ complex was uncertain.

The results of the treatment of the solubility data are presented in Table 2 and the molar absorptivities are summarized in Table 3. Examples of the absorption spectrum are shown in Figure 3 in which the solid curve represents the observed spectrum and the broken curve the calculated spectrum .

Table 2. Summary of the treatment of Scott and Hu's Solubility Data

$TlCl = Tl^{+} + Cl^{-}$ $K_1 = 0.25$

$TlCl_2^{-} = TlCl + Cl^{-}$ $K_2 = 1.87$

$TlCl_4^{\equiv} = TlCl_2^{-} + 2Cl^{-}$ $K_{4_c} = 93$

$TlCl_6^{-5} = TlCl_2^{-} + 4Cl^{-}$ $K_{6_c} = 1800$

Conc. of KCl, mole/liter	Solubility of TlCl x 10^3, mole/liter	Calculated x 10^3, mole/l					
		Tl^{+}	TlCl	$TlCl_2^{-}$	$TlCl_4^{\equiv}$	$TlCl_6^{-5}$	Sol. of TlCl
0.97	1.706	0.530	0.774	0.401			1.705
1.88	1.808	0.280	0.762	0.766			1.808
2.32	1.929	0.221	0.763	0.945			1.929
2.74	2.156	0.180	0.765	1.121	0.090		2.156
3.15	2.359	0.148	0.748	1.260	0.134	0.073	2.363
3.55	2.653	0.125	0.761	1.444	0.195	0.127	2.652

Table 3. Molar Absorptivity

wavelength, mμ	liter mole^{-1}cm^{-1}			
	Tl^{+}	TlCl	$TlCl_2^{-}$	$TlCl_4^{\equiv}$
220	3.1×10^3	3.4×10^3	1.0×10^3	0.00
230	1.2×10^3	3.8×10^3	3.1×10^3	1.1×10^3
240	0.12×10^3	2.0×10^3	4.5×10^3	2.0×10^3
245	0.00	0.50×10^3	4.7×10^3	3.2×10^3
250	0.00	0.00	3.5×10^3	4.7×10^3
255	0.00	0.00	2.0×10^3	5.25×10^3
260	0.00	0.00	1.0×10^3	4.3×10^3
265	0.00	0.00	0.50×10^3	2.65×10^3
270	0.00	0.00	0.23×10^3	1.1×10^3

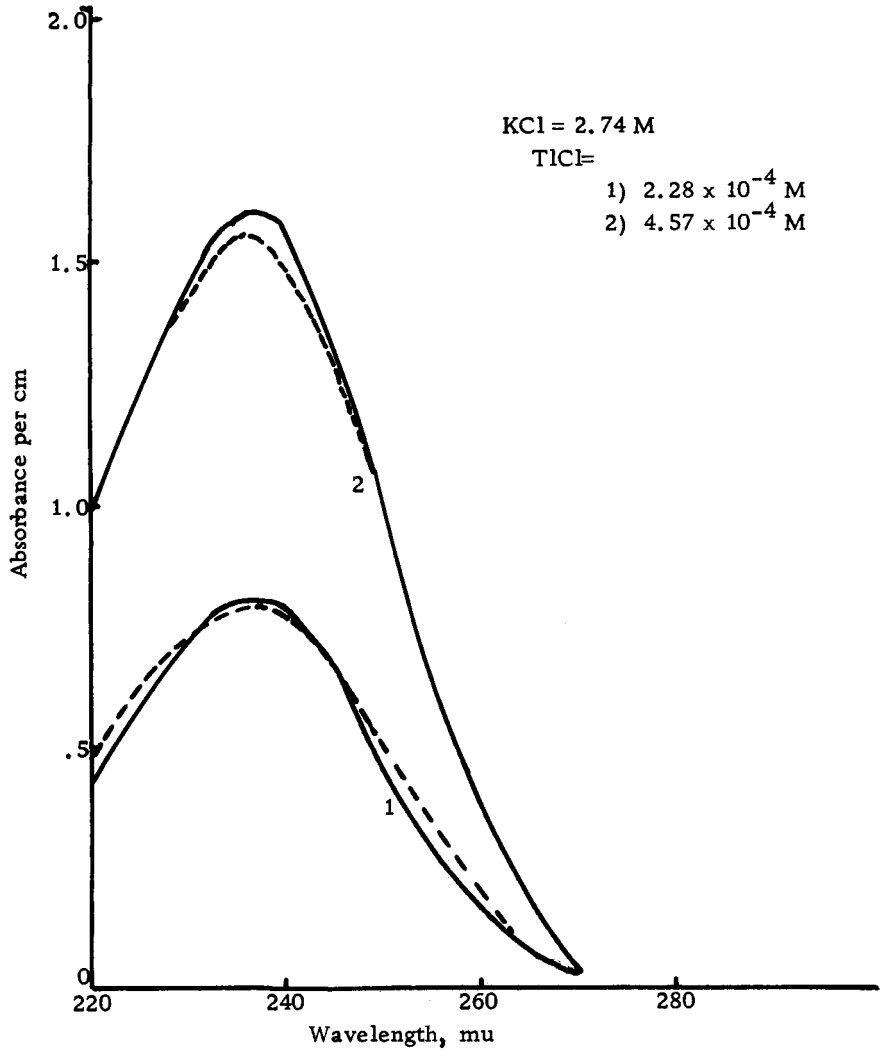

Figure 3. Absorption Spectrum of KCl solutions containing TlCl
Broken curves calculated; Solid curves observed data of Hu and Scott

2. KI:TlI solutions. In order to obtain formulas and dissociation constants for probable thallous iodide complexes, the solubility data of thallous iodide in potassium iodide due to Kul'ba (36) was treated according to the method of Hu and Scott (24). If the only complexes are TlI and TlI_2^-, then a plot of $(S - [Tl^+])$ vs. $[I^-]$ should be linear, with intercept $[TlI]$ and slope $\frac{[TlI]}{K_2}$. In contrast to the plots of $(S - [Tl^+])$ vs. $[Br^-]$ and $(S - [Tl^+])$ vs. $[Cl^-]$ which are linear up to halide ion concentrations of two molar, the plot for $(S - [Tl^+])$ vs. $[I^-]$, shown in Figure 4, is linear only up to I^- ion concentrations of 0.5 molar. The very pronounced upward curvature at concentrations greater than 0.5 molar suggests the existence of more highly coordinated thallous iodide complexes. For the

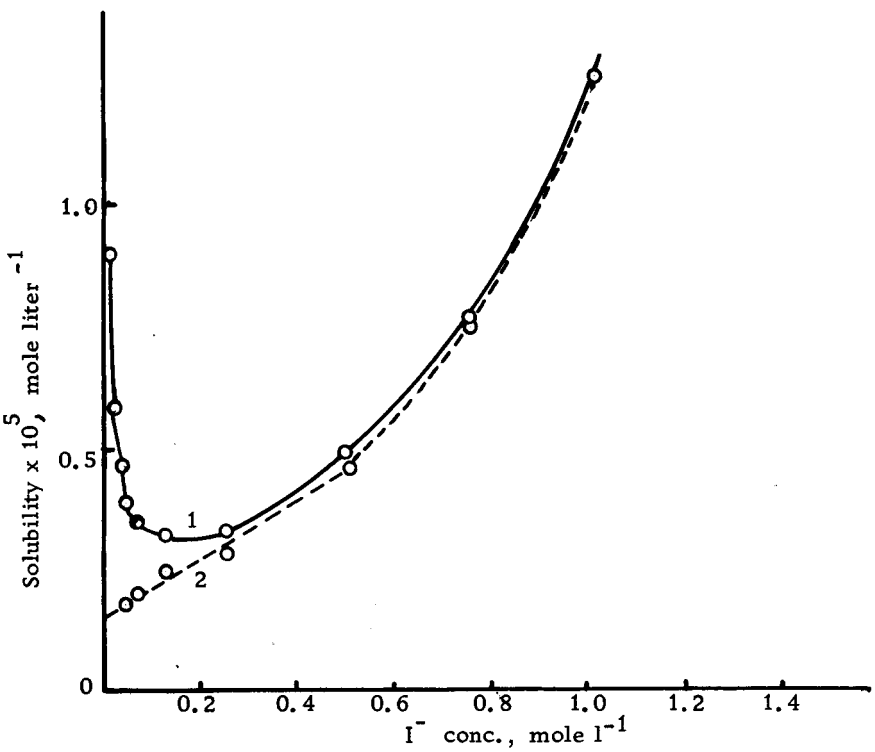

Figure 4. Curve 1. Solubility of TlI in KI solutions Curve 2. S- [Tl+]

calculation of the concentration of Tl^+ ion, the solubility product of TlI, 5.8×10^{-8}, as reported by Kul'ba, and the mean ionic activity coefficients $f_\pm$ of KI (20), corrected for volume concentrations, were used.

The intercept and slope of the linear portion of the plot were used to evaluate the dissociation constants for TlI and TlI_2^-

$$TlI = Tl^+ + I^- \qquad K_1 = \frac{[Tl^+][I^-] f_\pm^2}{[TlI]} = 0.034$$

$$TlI_2^- = TlI + I^- \qquad K_2 = \frac{[TlI][I^-]}{[TlI_2^-]} = 0.26$$

If the solubility in excess of that due to Tl^+, TlI, and TlI_2^- is assumed to be due TlI_3^{--} and TlI_4^{---} complexes, then the excess solubility, Δ, at a given I^- concentration will be given by

$$\Delta = \frac{[TlI_2^-][I^-]}{K_{3_c}} + \frac{[TlI_2^-][I^-]^2}{K_{4_c}}$$

where $K_{3_c} = \frac{[TlI_2^-][I^-]}{[TlI_3^{--}]}$ for the equilibrium $TlI_3^{--} = TlI_2^- + I^-$

and $K_{4_c} = \frac{[TlI_2^-][I^-]^2}{[TlI_4^{\equiv}]}$ for the equilibrium $TlI_4^{\equiv} = TlI_2^- + 2I^-$.

For each iodide ion concentration used, the excess solubility may be expressed as above. These equations were solved simultaneously resulting in a value of 2.0 for K_{3_c} and 3.5 for K_{4_c}.

The agreement between the calculated solubility and the experimental value found by Kul'ba is good except for the KI

concentration range 2.4 to 3.2 molar and for KI concentrations greater than 5.0 molar where more highly coordinated complexes are possibly TlI_5^{----} or TlI_6^{-----}. Presented in Table 4 is a comparison of the experimental solubilities, the calculated solubilities according to Kul'ba, and the solubilities calculated using the dissociation constants determined by the method of Hu and Scott.

Table 4. Solubility of thallous iodide in potassium iodide solutions

KI concentration, moles l^{-1}	Solubility of TlI x 10^5, moles $liter^{-1}$		
	Experimental (36)	Calculated (this work)	Calculated (Kul'ba)(36)
0.248	0.33	0.35	0.40
0.500	0.49	0.49	0.69
0.747	0.77	0.80	0.97
1.013	1.28	1.28	1.43
1.425	2.20	2.20	2.37
1.948	3.68	3.81	4.00
2.420	4.66	5.92	6.24
2.697	6.06	7.47	7.81
2.862	6.55	8.52	8.86
3.256	9.22	11.43	10.66
3.554	13.58	14.03	13.21
3.860	17.34	17.13	17.18
4.302	22.47	22.37	22.13
4.760	28.98	28.95	27.84
5.140	39.52	35.21	32.56
5.500	49.87	42.02	39.60

Kul'ba determined the composition and stability of the complex ions by drawing curves of the logarithm dependence of the solubility on the total iodide ion concentration. Tangents corresponding to all possible values of n were drawn to these curves and from the point of contact the concentration of iodide ion, for which $[TlI_n] = [TlI_{n+1}]$, was determined and instability constants were calculated. Complex ions of the following composition were determined: TlI, TlI_2^-, $TlI_3^=$, $TlI_4^{\equiv}$. The general equation for the instability constants, K_n, was expressed as

$$K_n = \frac{K_{sp}[I^-]^{n-1}}{[TlI_n^{-(n-1)}]} ,$$

where K_{sp} is the solubility product of TlI. For TlI, TlI_2^-, $TlI_3^=$, and $TlI_4^{\equiv}$, the instability constants are 0.0297, 0.0095, 0.0130, and 0.0418 respectively. Kul'ba's instability constants and the K_{3_c} and K_{4_c} dissociation constants given above are constants involving concentrations rather than activities, whereas K_1 and K_2 are, to a first approximation, thermodynamically correct constants.

The absorption spectra for KI:TlI solutions were difficult to measure. This was due to the fact that I_2, formed by oxidation, probably united with I^- ion to form the I_3^- ion. The solutions had a yellow tinge; however upon an addition of solid $Na_2S_2O_3 \cdot 10H_2O$, the solutions became colorless. According to Hersh (22), who studied the absorption spectra of aqueous KI solutions, initially colorless, to which I_2 had been added to give a yellow-brown color, the absorption of the I_3^- has strong maxima at 287 and 350 mμ as shown in

Figure 5. (22)

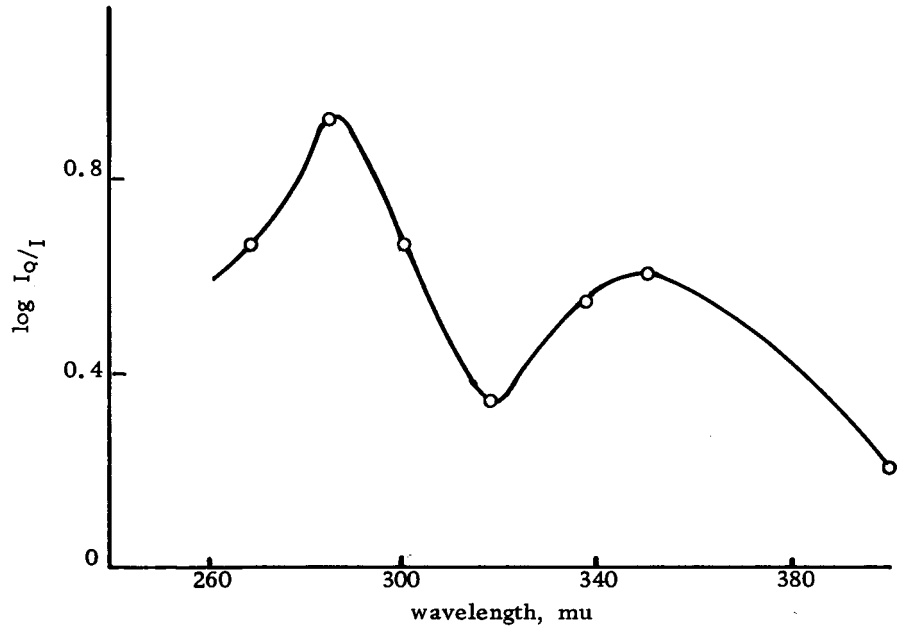

Figure 5. Absorption spectrum of I_2 in KI solution

The absorption spectra of KI:TlI solutions, in which the KI concentration was 0.5, 1.0, 2.0, 3.0, 4.0, and 5.0 moles liter^{-1} and the TlI concentrations ranged from zero to the solubility, were measured. In order to decolorize the solutions, $Na_2S_2O_3$ was added. The absorption spectra, representative samples of which are shown in Figure 6, exhibit maxima at approximately 270 and 300 mμ. The 300 mμ maximum was not noticeable in 0.5 molar or 1.0 molar KI solutions. This would suggest that the 300 mμ maximum is due to TlI_3^{--} and TlI_4^{---} complexes. The peak height and location of the 300 mμ maximum varies with both I^- and TlI concentration.

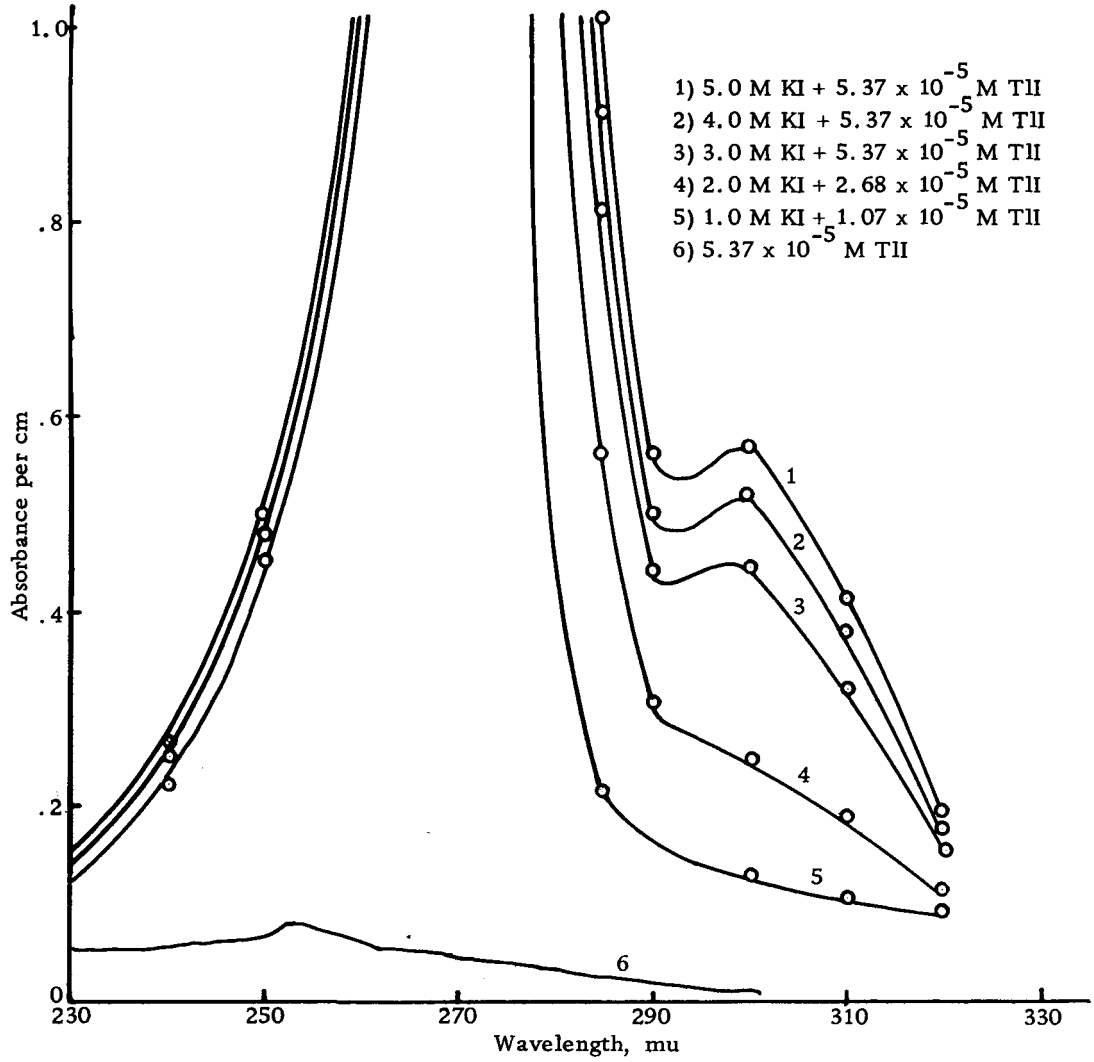

Figure 6. Absorption Spectra of KI: TlI solutions

If plots are made of the net absorbance per cm at I^- concentrations of 3.0, 4.0, and 5.0 molar against TlI_2^- concentration at wavelengths from 280 to 320 mμ, the curves should be linear and from the slopes of such curves the molar absorptivities of the complexes may be obtained. The plots of the absorbance per cm against

TlI_2^- concentration were not linear. More extensive experimental work is required in order to determine the effect of $Na_2S_2O_3$ and I_3^-, which still may be present, on the absorption spectra.

B. Excitation and Emission Spectra

1. General Remarks. The observed spectra obtained from the instrument used are apparent spectra and do not correspond to the true physical properties of the system. In order to obtain corrected spectra, certain factors were applied to observed data. These correction factors were obtained from a) the intensity of the exciting source as a function of frequency, b) the absorption of the excitation radiation by the solution, and c) the spectral response characteristics of the photomultiplier.

a) Xenon arc intensity as a function of wavelength.

The intensity of exciting radiation as a function of wavelength was determined by the potassium oxalatoferrate (III) chemical actinometer. The results are summarized in Figure 7 in which the flux in quanta/cm^2/sec is plotted against the wavelength of the exciting radiation. The cause of the peak at 290 mμ is unknown.

Since the center of the excitation band for most species involved in this investigation is at 250 mμ, the relative intensity at 250 mμ was taken as 1.00. Accordingly, the correction factors, presented in Table 5, were used. White and coworkers (65) have also determined relative intensities for the xenon arc in an Aminco-Bowman spectrophotofluorometer and these values are found in Table 5.

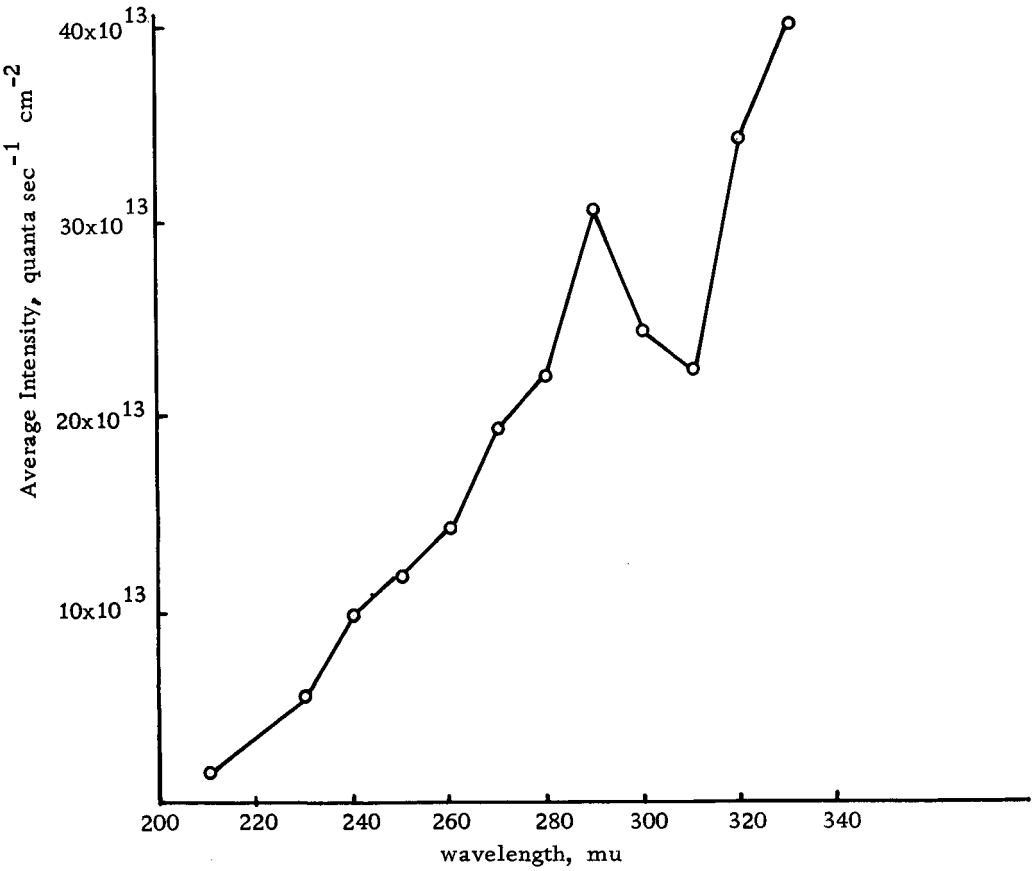

Figure 7. Average Xeon Arc Intensity as a function of wavelength. Determined by the potassium oxalato ferrate (III) actinometer.

Table 5. Relative intensity from excitation monochromator at constant slit width

Wavelength, mμ	Relative Intensity factor this work	White (65)
210	0.14	
220	0.30	
230	0.47	
240	0.82	0.80
250	1.00	1.02
260	1.19	1.35
270	1.64	1.70
280	1.86	2.00
290	2.60	2.28
300	2.06	2.61
310	1.97	3.00
320	2.89	3.38
330	3.36	3.70
340	3.75	4.10

These correction factors are applied by dividing the observed readings by the factor; the corrected spectra are then those which would be observed with constant excitation intensity.

b) Absorption of the excitation radiation

Presented in Figure 8 is a schematic drawing of the geometry of the cell compartment of the Aminco-Bowman Spectrophotofluorometer. The fluorescence radiation observed by the emission monochromator and photomultiplier is due to ions enclosed in the thin cross-hatched section in the center of the cell. The volume of this section (and hence the number of ions) is determined by the slit arrangement used. Due to absorption of the exciting radiation by the path length up to this section, the intensity of the exciting radiation for molecules enclosed in this section varies markedly from solution

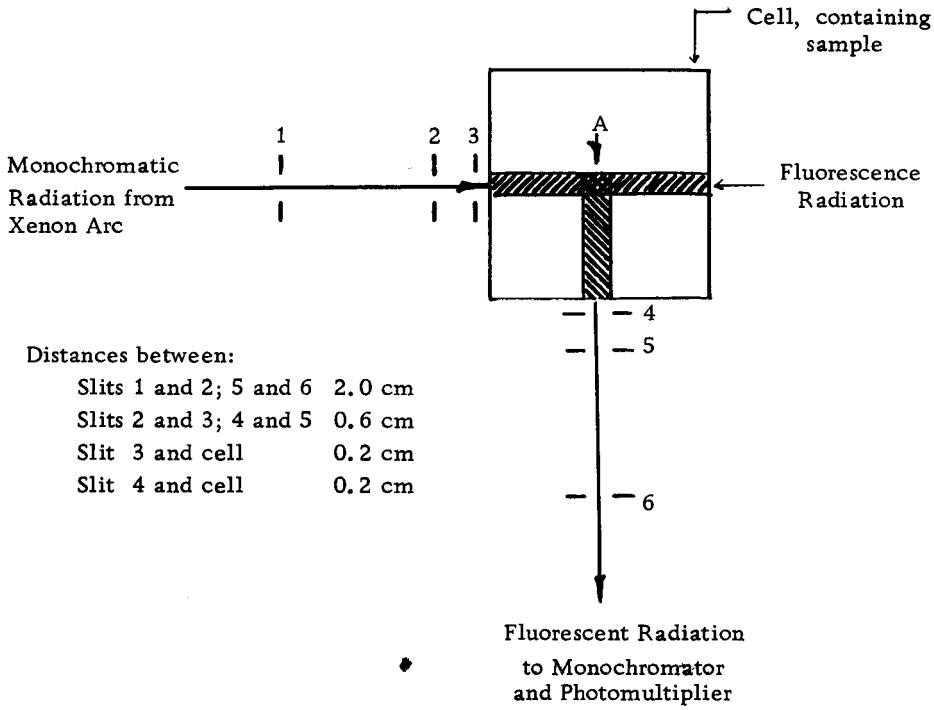

Figure 8. Geometry of the Aminco-Bowman Spectrophotofluorometer Cell Compartment, Top View

to solution. This decrease in intensity is illustrated in the adjoining table in which is tabulated the results of absorption calculations for KCl:TlCl solutions excited at 250 mμ with 1/16 inch defining slits.

Table 6. Transmittancy at point A of Figure 8 for KCl:TlCl solutions

Concentration	Transmittancy at Point A of Figure 8	Concentration	Transmittancy at Point A of Figure 8
0.25 M KCl+ 1.33×10^{-4} M TlCl	0.977 I_o	0.25 M KCl+ 2.67×10^{-4} M TlCl	0.958 I_o
0.50 M KCl+ " "	0.943 I_o	0.50 M KCl+ " "	0.894 I_o
1.00 M KCl+ " "	0.878 I_o	1.00 M KCl+ " "	0.782 I_o
2.00 M KCl+ " "	0.787 I_o	2.00 M KCl+ " "	0.638 I_o
3.00 M KCl+ " "	0.717 I_o	3.00 M KCl+ " "	0.536 I_o
4.00 M KCl+ " "	0.641 I_o	4.00 M KCl+ " "	0.433 I_o

Thus a direct comparison of the observed photomultiplier readings is valid only when the optical densities of the solutions being compared are equal. Accordingly, a correction was applied to all readings so that they were those which would have resulted from equal exciting intensities entering the section.

c) Spectral Response Characteristics of the photomultiplier

The final correction that was applied was determined by the spectral response of the photomultiplier detector used. Since an RCA type IP-28 photomultiplier was used for all observations, the S-5 spectral sensitivity curve as published by RCA (50) was used to correct the observed readings. The corrections were made by dividing the observed readings by the relative sensitivity, expressed as a fraction, at the emission wavelength under consideration.

All spectra denoted as "corrected" have had the above correction factors applied and those spectra denoted as "uncorrected" are observed spectra.

2. Excitation and Emission Characteristics of KCl:TlCl solutions. The hydrated thallous ion (as in aqueous solutions of TlCl, TlBr, Tl_2CO_3, and $TlNO_3$) has an absorption maximum at 215 mμ and a fluorescent maximum at 370 mμ. If chloride ion is added to solutions containing the thallous ion, the absorption and emission maxima shift toward longer wavelengths. Presented in Figure 9 are the corrected and uncorrected excitation spectra for representative KCl:TlCl solutions. In these curves the total thallium content is

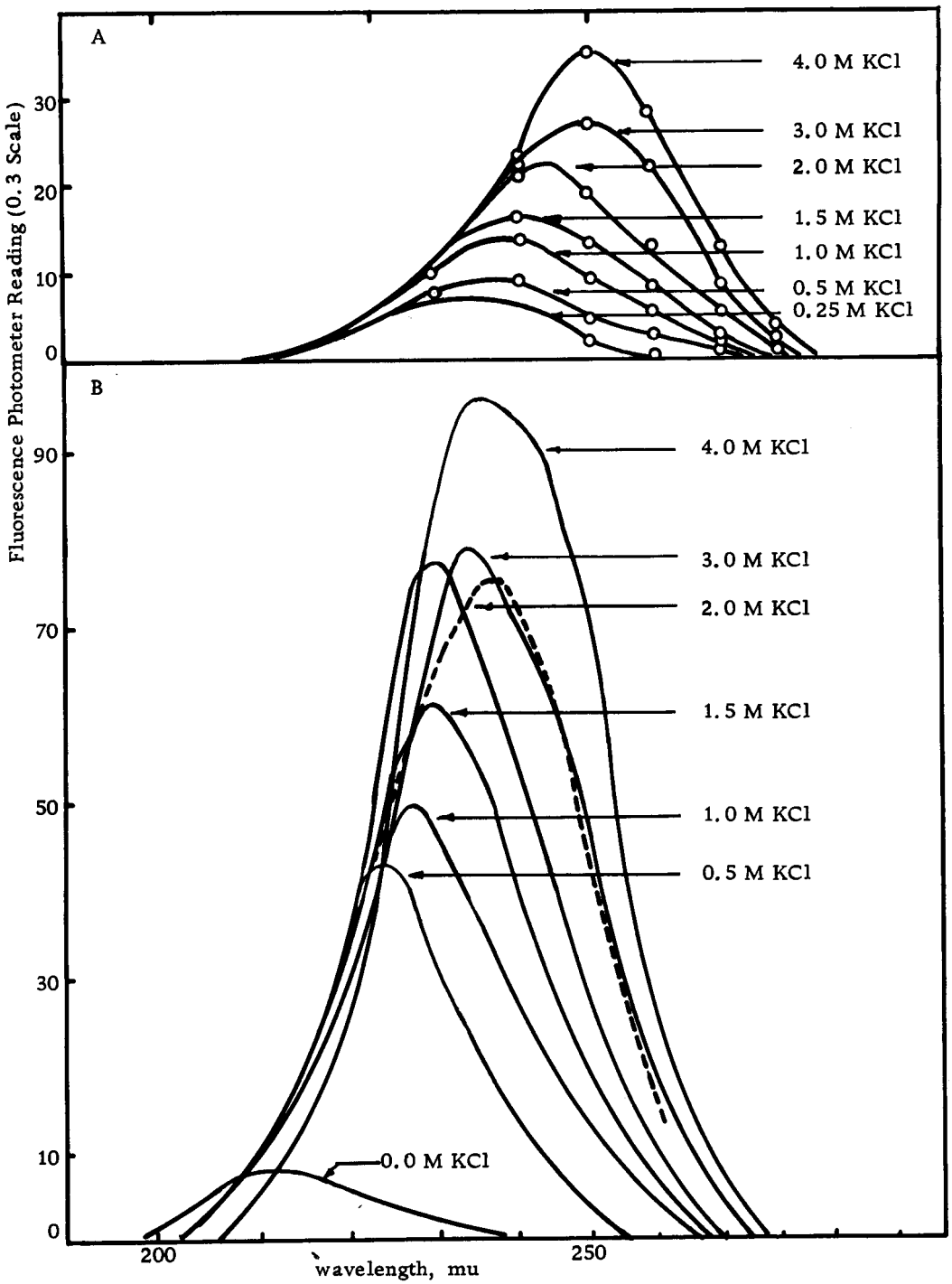

Figure 9. Excitation Spectra, 430 mu Emission$_x$ for KCl solutions containing 1.33×10^{-4} M TlCl

A. Uncorrected B. Corrected

Dotted line: Normalized absorption for 3.0 M KCl solution

constant and the concentration of KCl was varied. The shift of the excitation peak towards longer wavelengths accompanied by the change in peak height with increasing chloride ion concentration furnishes evidence of complex ion formation. The close correspondence of the corrected excitation spectrum with the corresponding absorption spectrum, represented by a dotted line in Figure 9B, probably is indicative that all complex species are fluorescing.

The emission spectra of KCl:TlCl solutions consist of a broad band with maximum at 435-440 $m\mu$. KCl solutions, to which no TlCl has been added, did not fluoresce observably. Presented in Figure 10 are representative corrected and uncorrected emission spectra for KCl:TlCl solutions in which the total thallium content is constant. The shift in maximum from the 370 $m\mu$ emission characteristic of the hydrated thallous ion to 430 $m\mu$, characteristic of the complexes, as well as the simultaneous change in peak height with increasing chloride ion concentration is indicative that complex ions have formed and are responsible for the fluorescence. At chloride ion concentrations greater than 0.5 M, the location of the emission maximum no longer changes with concentration.

Pringsheim (48, 49) has reported the simultaneous appearance of an ultraviolet fluorescent band with maximum at 300 $m\mu$ and with an intensity one-twentieth that of the visible band. Careful examination of the ultraviolet portion of the spectrum did not reveal the presence of this band.

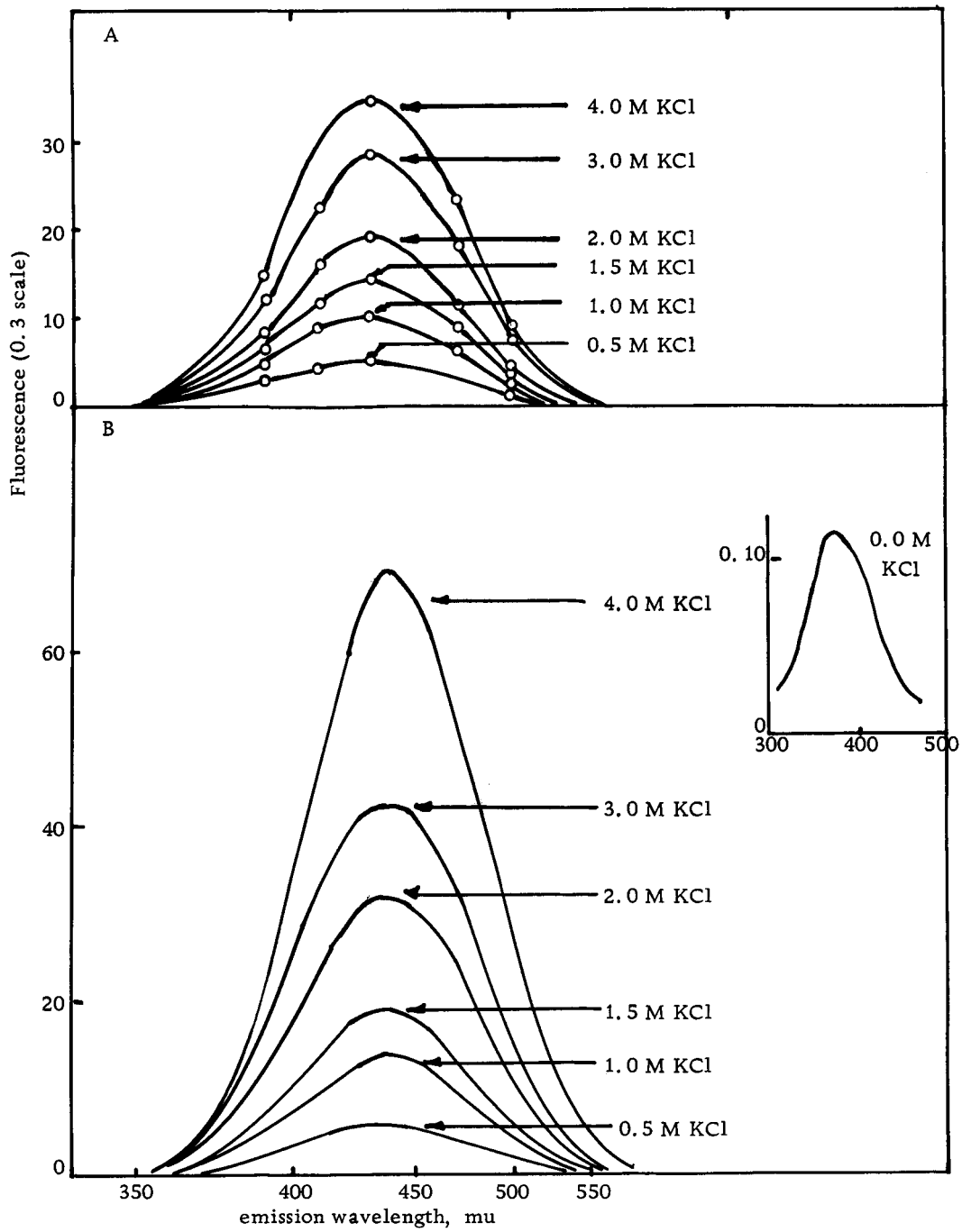

Figure 10. Emission Spectra, 250 mu Excitation, for KCl Solutions containing 1.33 x 10^{-4} M TlCl

A. Uncorrected B. Corrected

Pringsheim (49) also reported that he found differences between freshly prepared solutions and solutions which had "aged" at least two days. Very little noticeable difference was found in solutions that were observed on the same day that they were prepared as compared to readings taken several days later.

For all KCl:TlCl solutions, the fluorescence intensity increases with increasing TlCl concentration; however at total thallium concentrations greater than 2.67×10^{-4} M, the "optimum concentration", the uncorrected fluorescence decreases. At extremely high concentrations, i.e. 1.334×10^{-3} M TlCl, the fluorescence as indicated by the photomultiplier photometer is reduced many fold; however if a visual observation is made, the fluorescence is extremely bright at the front surface of the cell and fans out into a very weak band from the front surface. If, however, the photomultiplier photometer readings are corrected for internal absorption of the exciting radiation, then it was found that the fluorescence intensity increases with increasing thallium chloride content beyond the optimum concentration. Shown in Figure 11 are the corrected and uncorrected fluorescence intensities plotted against the logarithm of the total thallium content.

Summarized in the adjoining table are the observed locations of the excitation and emission maxima for representative KCl:TlCl solutions.

Table 7. Location of the observed excitation and emission maximum for KCl solutions containing 5.26×10^{-4} M TlCl

KCl Concentration, mole/liter	Excitation maximum, mμ	Emission maximum, mμ
0	225	365
0.005	225	390
0.01	230	405
0.25	235	425
0.50	240	430
1.0	245	430
2.0	250	430
3.0	250	430
4.0	255	430

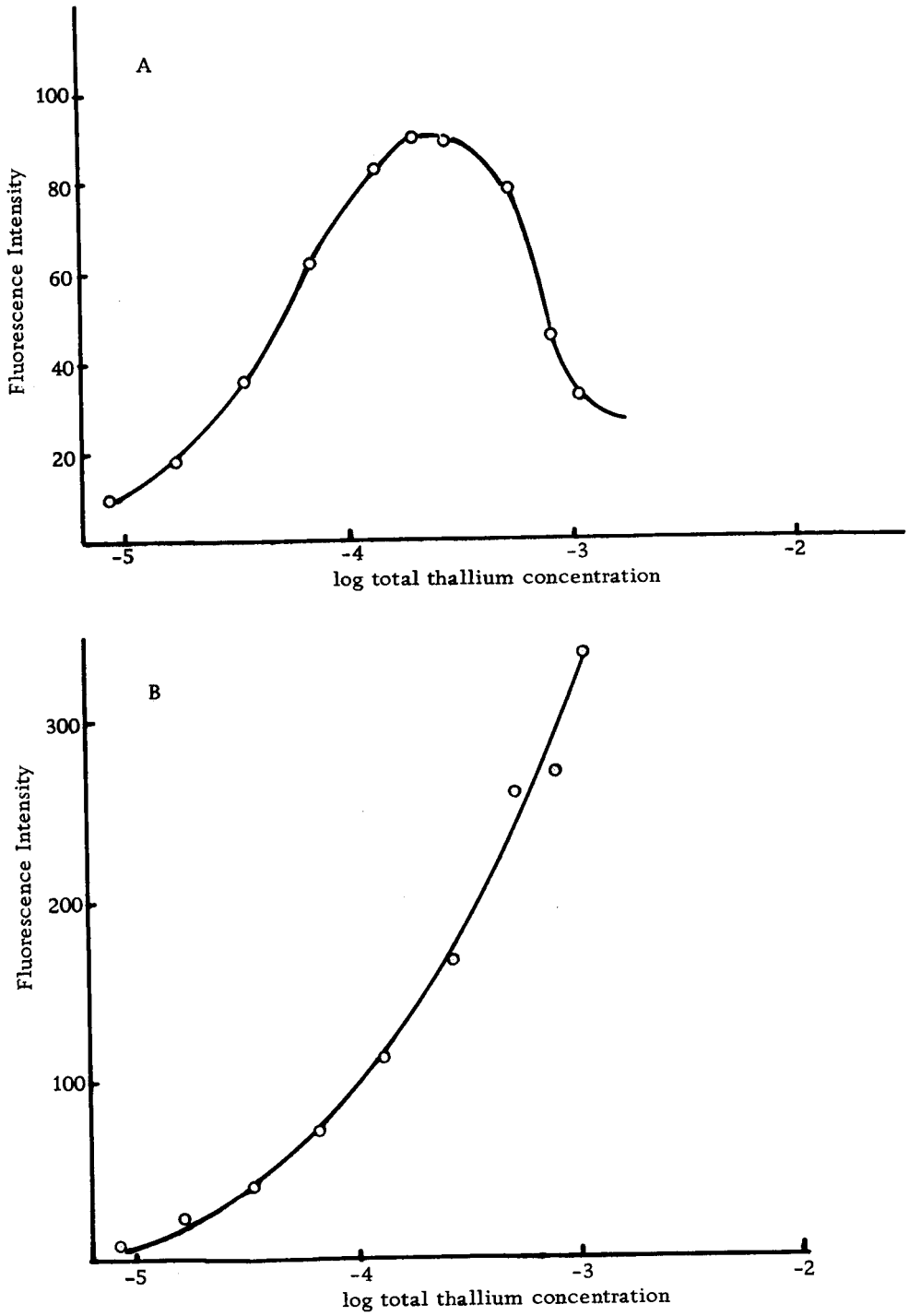

Figure 11. Fluorescence intensity as a function of the logarithm of the total Tl concentration for 3.0 M KCl solutions, 250 mu Excitation, 430 mu Emission

A. Uncorrected B. Corrected

3. Excitation and Emission Characteristics of KBr:TlBr solutions. Presented in Figure 12 are the observed and corrected excitation spectra for representative KBr:TlBr solutions. There is a marked similarity to the KCl:TlCl solution; the excitation spectra exhibit a similar shift of the excitation maximum and change in peak height with increasing bromide concentration. The close parallel between the absorption, represented by a dotted line in Figure 12B, and excitation spectrum suggests that TlBr, $TlBr_2^-$, and $TlBr_4^{\equiv}$ complexes are the luminescence centers.

The vivid blue-green fluorescence of KBr:TlBr solutions consists of a broad band with maxima at 470 $m\mu$. The corrected and uncorrected emission spectra for representative KBr:TlBr solutions are shown in Figure 13. Since there is no shift in the location of the band maximum with bromide solutions 0.5 M and greater, the TlBr, $TlBr_2^-$, and $TlBr_4^{\equiv}$ luminescence centers evidently fluoresce in the same spectral region.

Pringsheim (49) reported the existence of a weak ultraviolet band with maximum at 320 $m\mu$ but Shinoya et al. (58) failed to confirm Pringsheim's observations. No emission band was observed in the region between 300 and 400 $m\mu$.

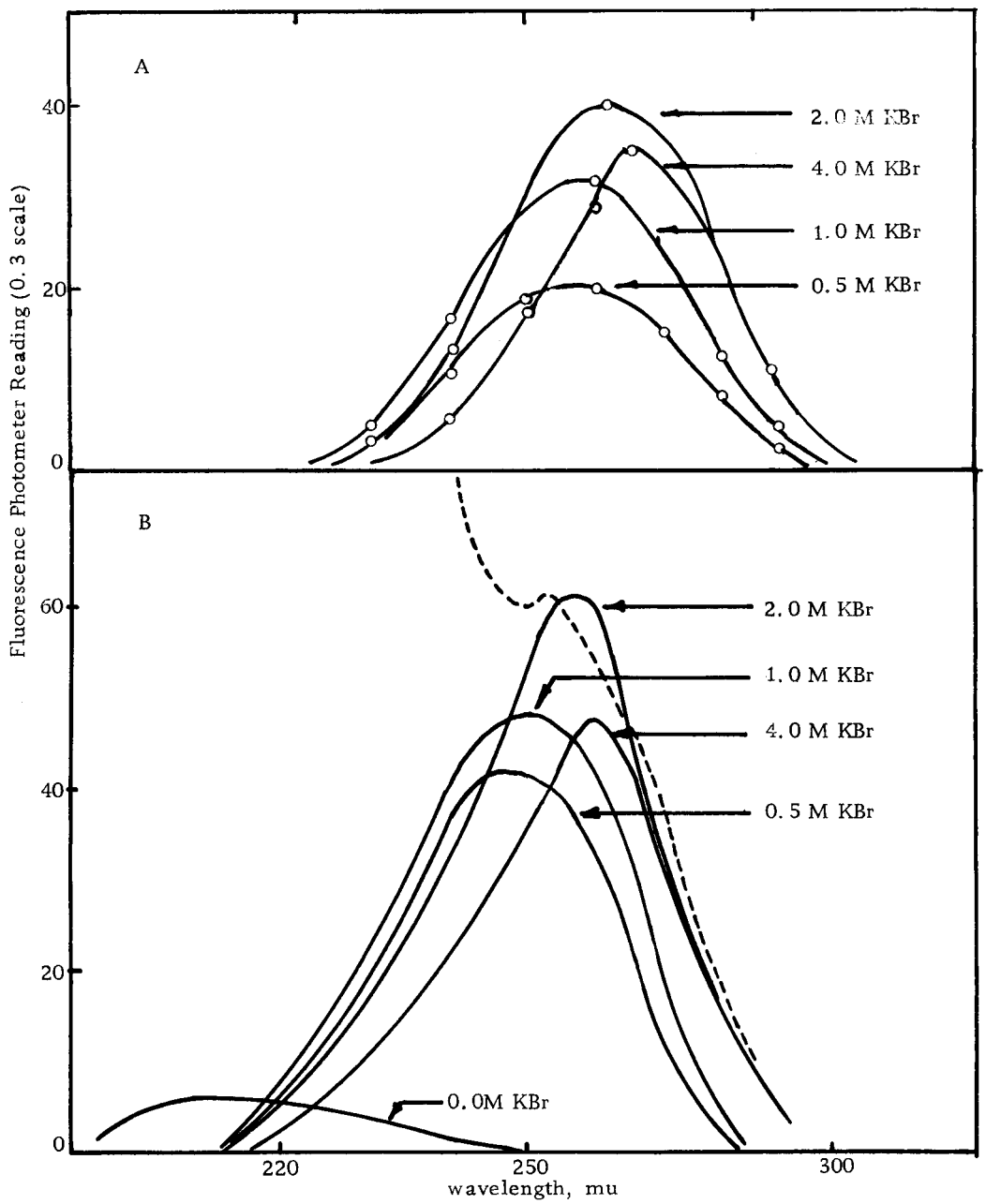

Figure 12. Excitation Spectra, 470 mu Emission, for KBr solutions containing 2.67 x 10^{-5} M TlBr

A. Uncorrected B. Corrected

Dotted line: Indicates the absorption spectrum of 1.87 M KBr solution

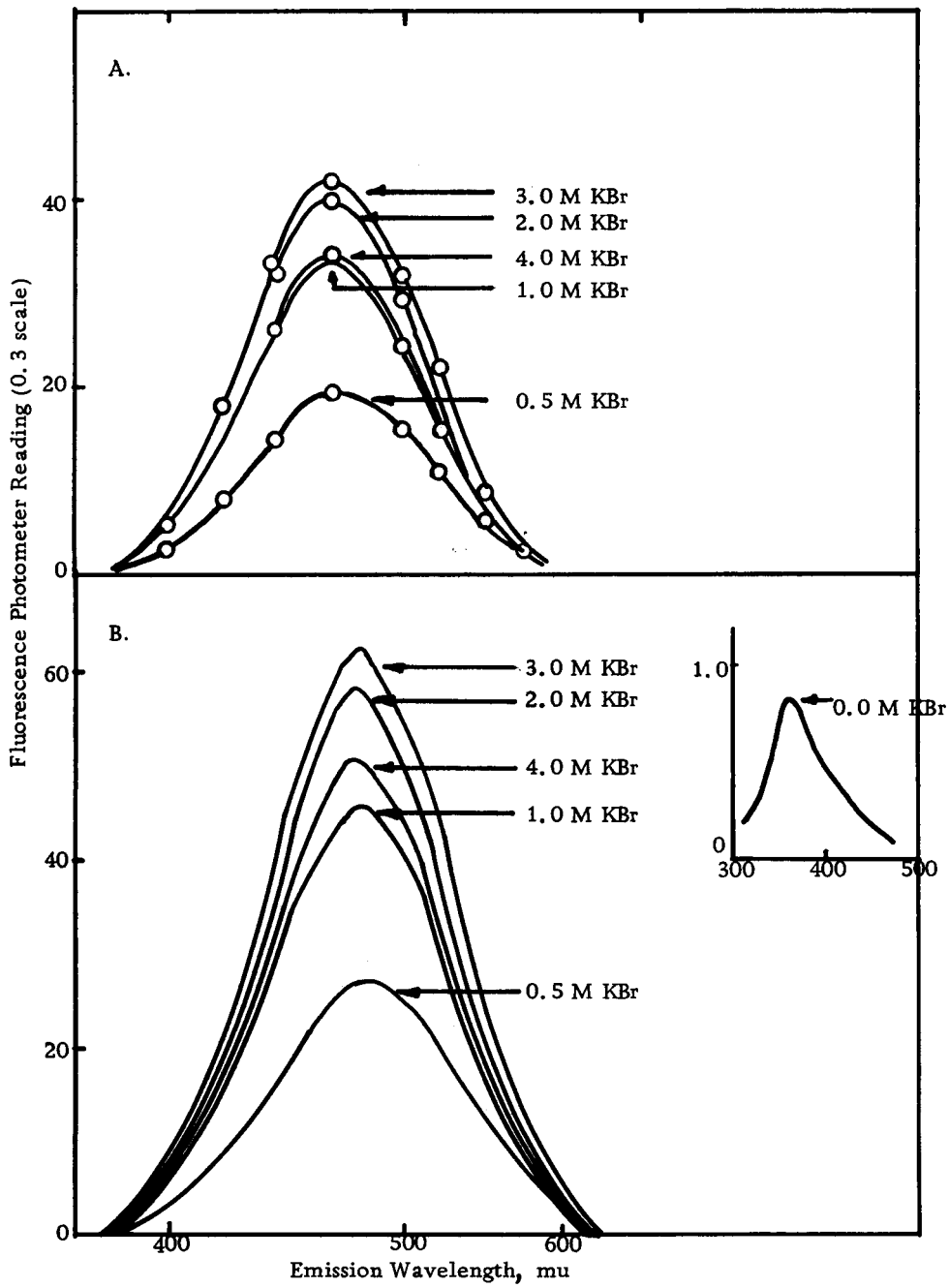

Figure 13. Emission Spectra, 260 mu Excitation, for KBr solutions containing 2.67×10^{-5} M TlBr

A. Uncorrected
B. Corrected

4. Excitation and Emission Characteristics of KI:TlI solutions. In contrast to the vivid fluorescence of KCl:TlCl and KBr:TlBr solutions, the KI:TlI solutions were found to fluoresce weakly. The emission spectra were complicated by the fact that since the widest slits available were used, the background scatter from the solution was very high. A second complication arises from the scattered light from the second order diffraction of the original exciting source; this scattered light appears in the same spectral region as the emission spectrum of KI:TlI solutions.

The observed excitation and emission spectra for KI:TlI solutions are presented in Figure 14. The excitation spectra have maxima at 280 mμ for 0.5 M KI solutions shifting to 300 mμ for 5.0 M KI solutions. The emission spectrum is composed of a weak, broad band with maximum at 500-520 mμ .

Since the initially colorless KI:TlI solutions rapidly acquired a characteristic yellow-brown hue, $Na_2S_2O_3$ was added to repress the formation of I_3^-. Emission and excitation spectra were recorded before and after the addition. As shown in Figure 15, the effect of $Na_2S_2O_3$ addition is a slight enhancement of the peak height with no appreciable shift in peak location.

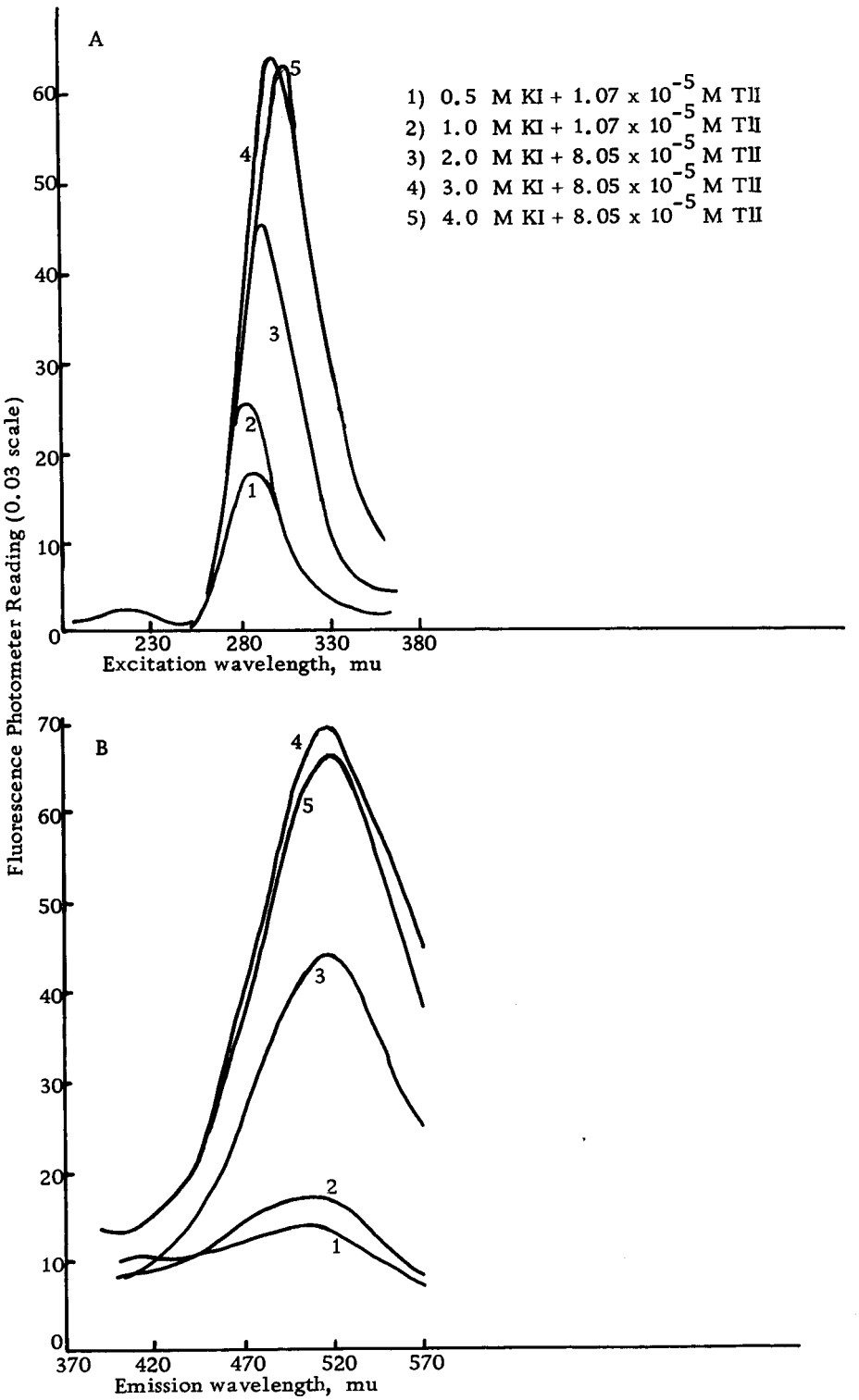

Figure 14. Excitation and emission spectra of KI: TlI solutions
A. Excitation Spectra, 500 mu Emission
B. Emission Spectra, 300 mu Excitation

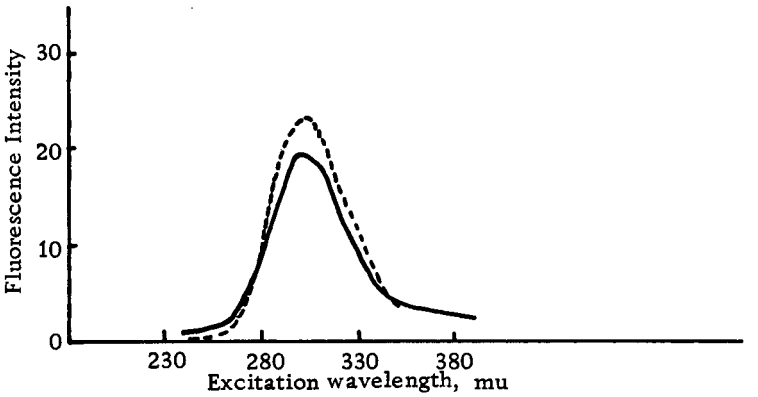

Effect of adding $Na_2S_2O_3$ to 3.0M KI + 8.06×10^{-5} M TlI solution

Excitation Spectra, 500 mu Emission

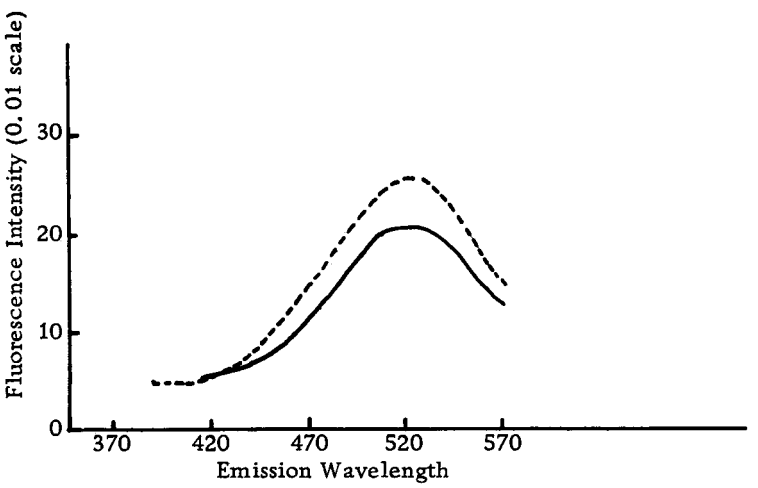

Effect of adding $Na_2S_2O_3$ to 3.0 M KI + 8.06×10^{-5} M TlI solution

Emission Spectra, 300 mu Excitation

Solid line: Before addition
Dotted line: $Na_2S_2O_3$ added

Figure 15

C. Analysis of the Emission Spectra

The concentration of each species present was computed using the dissociation constants and equilibrium equations for the complexes. Consider the following equilibria and dissociation constants:

$$TlCl = Tl^{+} + Cl^{-} \; ; \quad K_1 = \frac{[Tl^{+}][Cl^{-}]}{[TlCl]} f_{\pm}^{2} = 0.25$$

$$TlCl_2^{-} = TlCl + Cl^{-} \; ; \quad K_2 = \frac{[TlCl][Cl^{-}]}{[TlCl_2^{-}]} = 1.87$$

$$TlCl_4^{\equiv} = TlCl_2^{-} + 2Cl^{-} \; ; \quad K_{4_c} = \frac{[TlCl_2^{-}][Cl^{-}]^2}{[TlCl_4^{\equiv}]} = 93$$

$$TlCl_6^{-5} = TlCl_2^{-} + 4Cl^{-} \; ; \quad K_{6_c} = \frac{[TlCl_2^{-}][Cl^{-}]^4}{[TlCl_6^{-5}]} = 1800 \; .$$

The concentration of $TlCl_2^{-}$ is given by

$$[TlCl_2^{-}] = \frac{t}{\left[\frac{z^4}{K_{6_c}} + \frac{z^2}{K_{4_c}} + 1 + \frac{K_1 K_2}{z^2 f_{\pm}^2} + \frac{K_2}{z}\right]} \; ,$$

where t is the total thallium concentration, z is the chloride ion concentration, and $f_{\pm}$ is the mean ionic activity coefficient. The mean ionic activity coefficients are those reported by Harned (20) and were corrected for use with volume concentrations.

The concentrations of the other species present are given by

$$[TlCl_6^{-5}] = \frac{z^4}{K_{6_c}} [TlCl_2^{-}]$$

$$[TlCl_4^{\equiv}] = \frac{z^2}{K_{4_c}} [TlCl_2^{-}]$$

$$[TlCl] = \frac{K_2}{z}[TlCl_2^-]$$

$$[Tl^+] = \frac{K_1K_2}{z^2f_\pm^2}[TlCl_2^-]$$

Similarly, the concentration of each species in KBr:TlBr solutions was ascertained considering the following equilibria and dissociation constants (56):

$$TlBr = Tl^+ + Br^- \qquad K_1 = \frac{[Tl^+][Br^-]f_\pm^2}{[TlBr]} = 0.24$$

$$TlBr_2^- = TlBr + Br^- \qquad K_2 = \frac{[TlBr][Br^-]}{[TlBr_2^-]} = 0.30$$

$$TlBr_4^{\equiv} = TlBr_2^- + 2Br^- \qquad K_{4_c} = \frac{[TlBr_2^-][Br^-]^2}{[TlBr_4^{\equiv}]} = 16 .$$

Summarized in Table 8 are the results of the concentration calculation for KCl:TlCl and KBr:TlBr solutions.

Table 8. Summary of Concentrations

a) KCl:TlCl solutions t = total thallium (I) concentration

	Tl^+	TlCl	$TlCl_2^-$	$TlCl_4^{\equiv}$	$TlCl_6^{-5}$
0.25 M KCl	0.64 t	0.32 t	0.04 t		
0.50 M KCl	0.48 t	0.41 t	0.11 t		
1.0 M KCl	0.30 t	0.45 t	0.24 t		
1.5 M KCl	0.20 t	0.44 t	0.35 t		
2.0 M KCl	0.14 t	0.41 t	0.44 t		
3.0 M KCl	0.07 t	0.34 t	0.54 t	0.05 t	
4.0 M KCl	0.03 t	0.25 t	0.54 t	0.09 t	0.08 t

b) KBr:TlBr solutions

	Tl^+	TlBr	$TlBr_2^-$	$TlBr_4^{\equiv}$
0.5 M KBr	0.30 t	0.26 t	0.44 t	
1.0 M KBr	0.12 t	0.20 t	0.68 t	
2.0 M KBr	0.03 t	0.10 t	0.69 t	0.17 t
3.0 M KBr	0.01 t	0.06 t	0.60 t	0.33 t
4.0 M KBr	0.00 t	0.04 t	0.48 t	0.48 t

The emitted flux, F, for KCl:TlCl solution at any given excitation and emission wavelength is equal to the sum of the fluxes for each species, that is

$$F = F_0 + F_1 + F_2 + F_4 + F_6 \quad ,$$

where the subscripts denote the number of chloride ions coordinated with the thallium. At low concentrations, as developed on page 4, the fluorescence of a species, for example Tl^+, may be written as

$$F_0 = I_x \phi_0 \epsilon_0 c_0 \cdot$$

Letting $y_n = I_x \phi_n \epsilon_n$

then $F_n = y_n c_n$

and $F = y_0 c_0 + y_1 c_1 + y_2 c_2 + y_4 c_4 + y_6 c_6$

The above equation may be combined with the concentration equations on page 53 and 54 to give

$$F = [TlCl_2^-]\left[\frac{z^4}{K_{6_c}} y_6 + \frac{z^2}{K_{4_c}} y_4 + y_2 + \frac{K_2}{z} y_1 + \frac{K_1 K_2}{z^2 f_\pm^2} y_0\right]$$

The corrected fluorescence intensity, which will be symbolized F', is actually proportional to the flux of emitted <u>energy</u>, whereas F is the flux in photons per unit time. Letting

$$F' = \beta_1 \beta_2 F$$

where β_1 is a constant, which takes into consideration the geometry

of the spectrophotofluorometer, and β_2 is the energy per photon at the given wavelength. The corrected fluorescence intensity was plotted against the $TlCl_2^-$ concentration for a series of solutions at constant z at a given excitation and emission wavelength. The slope, equal to

$$\beta_1\beta_2 \left[\frac{z^4}{K_{6_c}} y_6 + \frac{z^2}{K_{4_c}} y_4 + y_2 + \frac{K_2}{z} y_1 + \frac{K_1K_2}{z^2 f_\pm^2} y_0 \right] ,$$

should be constant if the y's do not vary with concentration. Corresponding to each value of z will be a slope and the linear equations determined by the slopes may be solved simultaneously to obtain values for $\beta_1\beta_2 y_n$. Values for $\beta_1\beta_2 y_0$ were obtained from the emission spectra of dilute TlCl solutions, in which association is negligible.

Plots of F' against $TlCl_2^-$ concentration for z = 0.25, 0.5, 1.0, 2.0, 3.0, and 4.0 M at 230 mμ and 250 mμ excitation and 430 mμ emission are presented in Figure 16. Similar plots were prepared for emission at 400, 450, and 470 mμ emission and excitation at 230 and 250 mμ. The $\beta_1\beta_2 y_n$ values obtained by the method outlined above are presented in Table 9.

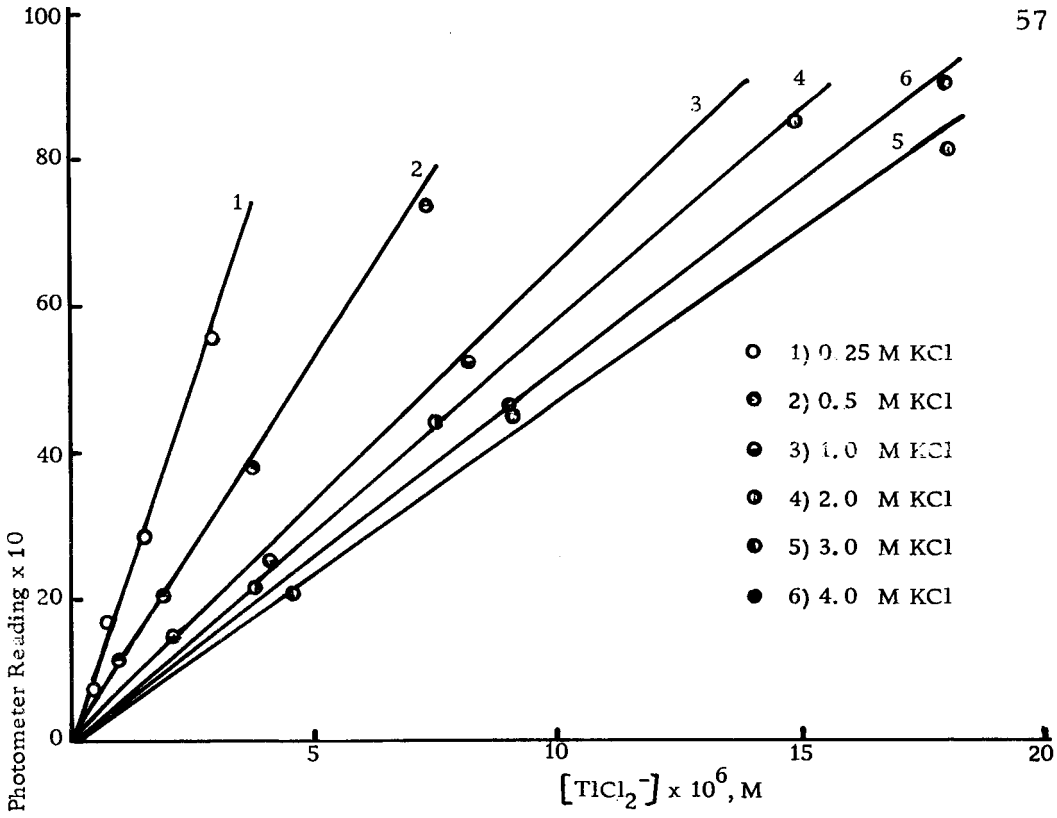

230 mu Excitation. 430 mu Emission

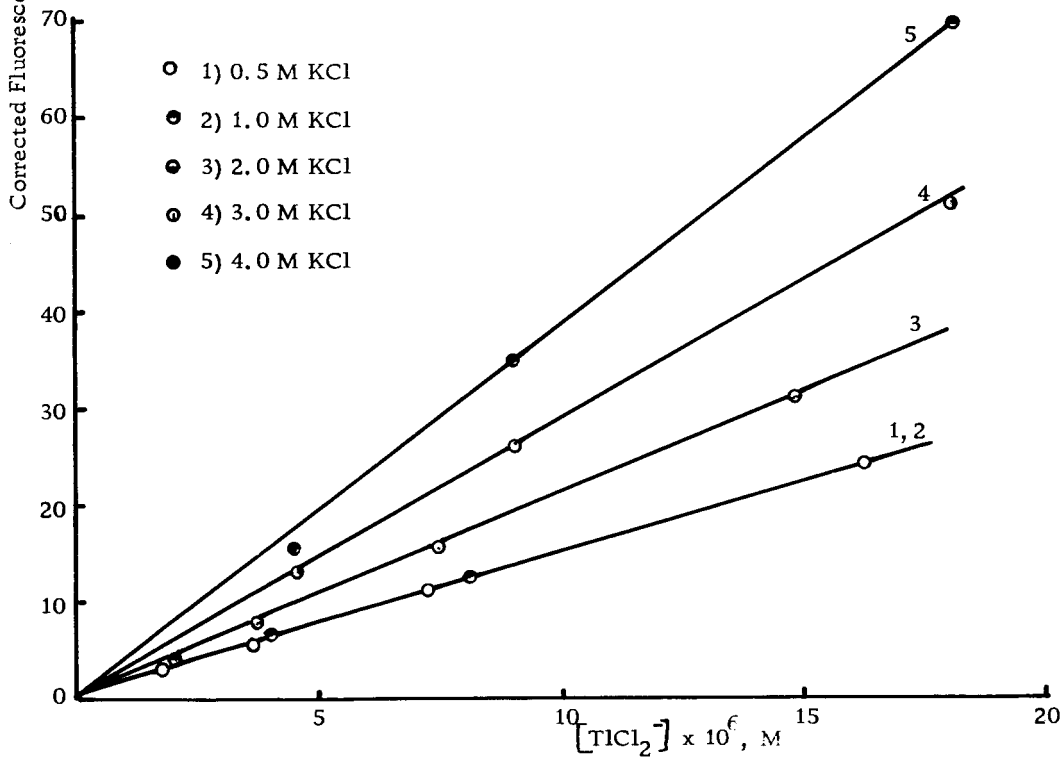

250 mu Excitation. 430 mu Emission

Figure 16. Variation of emission intensity with $TlCl_2^-$ concentration

Table 9. $\beta_1\beta_2 y_n$ values calculated from plots of F' against $TlCl_2^-$ concentration

a) 230 mμ Excitation

Emission wavelength, mμ	Tl^+	TlCl	$TlCl_2^-$	$TlCl_4^{\equiv}$	$TlCl_6^{-5}$
400	1.5×10^5	1.1×10^6	1.8×10^6	2.5×10^6	0
430	5.7×10^4	2.3×10^6	2.7×10^6	7.0×10^6	0
450	2.8×10^4	2.0×10^6	2.6×10^6	9.1×10^6	0
470	0	1.7×10^6	2.3×10^6	8.5×10^6	0

b) 250 mμ Excitation

Emission wavelength, mμ	Tl^+	TlCl	$TlCl_2^-$	$TlCl_4^{\equiv}$	$TlCl_6^{-5}$
400	0	0	1.2×10^6	4.3×10^6	
430	0	0	2.1×10^6	7.4×10^6	2.3×10^6
450	0	0	2.1×10^6	8.9×10^6	1.7×10^6
470	0	0	1.6×10^6	7.5×10^6	1.3×10^6

Since $y_n = I x \epsilon_n \phi_n$ and I, x, β_1, β_2 are all constant, the ratio $\beta_1\beta_2 y_n/\epsilon_n$ will be proportional to the quantum yield, ϕ_n. The $\beta_1\beta_2 y_n/\epsilon_n$ ratios were plotted against the emission wavelength and symmetric curves were drawn through the points. The plots are presented in Figure 17. The fluorescence emission maximum is located at 370 mμ for Tl^+, 435-440 mμ for TlCl and $TlCl_2^-$, and 450 mμ for $TlCl_4^{\equiv}$. From the plots presented in Figure 17, it may be seen that the fluorescence quantum yields for TlCl and $TlCl_2^-$ are approximately the same, whereas the quantum yield for $TlCl_4^{\equiv}$ is larger and that of Tl^+ is smaller than the quantum yield for TlCl or $TlCl_2^-$.

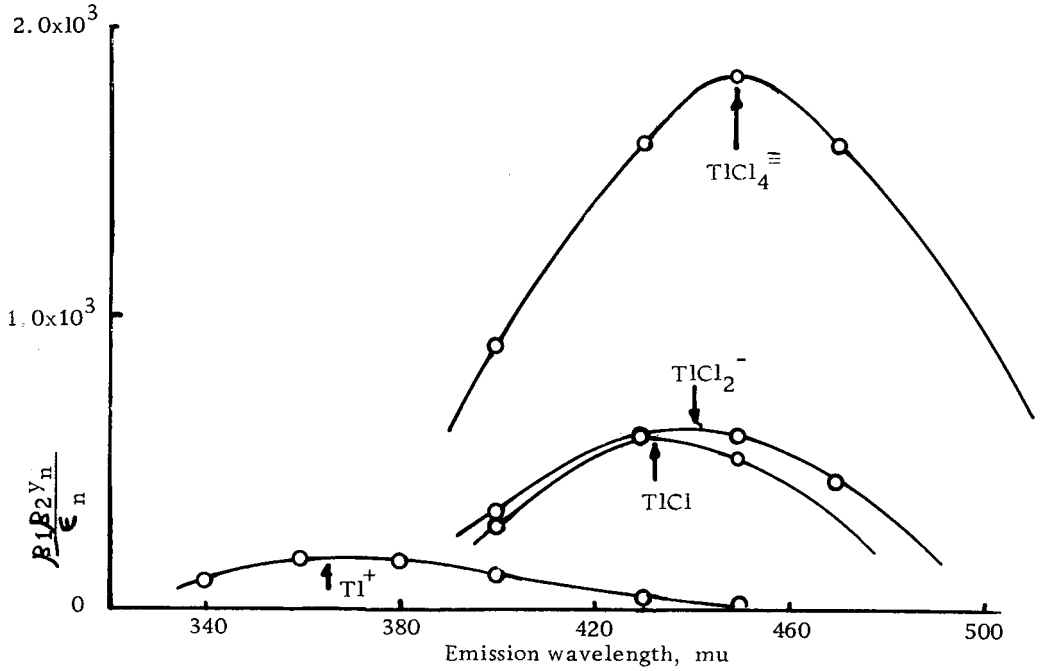

Figure 17. Variation of $\beta_1\beta_2 Y_n / \epsilon_n$ with emission wavelength for KCl:TlCl solutions

A comparison of the wavelengths of the emission maxima reported by Avramenko and Belyi (2) and by Brauer and Pelte (7) with those reported above is shown in Table 10.

Table 10. Wavelengths of the emission maximum for species present in KCl:TlCl solutions

Species	Wavelength of emission maximum, mμ		
	this work	Brauer (7)	Avramenko (2)
Tl^+	370	368	380
TlCl	435	395	428
$TlCl_2^-$	435	440	
$TlCl_4^{\equiv}$	450		428

The values of $\beta_1 \beta_2 y_n$ may be used in conjunction with the concentration of each species to calculate the percentage of the fluorescence which is due to each species. These percentage values are presented in Table 11.

Table 11. Percent fluorescence due to species present in KCl:TlCl solutions

a) 230 mμ Excitation, 430 mμ Emission

KCl Conc., mole/liter	Tl^+	TlCl	$TlCl_2^-$	$TlCl_4^{=}$
		Percent fluorescence due to		
0.25	4	83	13	0
0.5	2	74	23	0
1.0	1	61	38	0
1.5	0	51	48	0
2.0	0	44	56	0
3.0	0	30	56	14
4.0	0	22	54	22

b) 250 mμ Excitation, 430 mμ Emission

KCl Conc., mole/liter	Tl^+	TlCl	$TlCl_2^-$	$TlCl_4^{=}$	$TlCl_6^{-5}$
		Percent fluorescence due to			
0.5	0	0	100	0	0
1.0	0	0	100	0	0
1.5	0	0	100	0	0
2.0	0	0	100	0	0
3.0	0	0	75	25	0
4.0	0	0	57	34	9

The emission spectra of KBr:TlBr solutions were analyzed by the same procedure. The emitted flux at a given excitation and emission wavelength is given by

$$F = F_0 + F_1 + F_2 + F_4 .$$

At low concentrations, letting

$$y_n = Ix \epsilon_n \phi_n$$

and combining with the concentration expression for each species, then F is expressed by the following

$$F = [TlBr_2^-]\left[\frac{z^2}{K_{4_c}} y_4 + y_2 + \frac{K_2}{z} y_1 + \frac{K_1 K_2}{z^2 f_{\pm}^2} y_0\right] ,$$

where z is the bromide ion concentration, $f_{\pm}$ is the mean ionic activity coefficient for KBr corrected for use with volume concentrations, and the K's are the dissociation constants reported by Scott et al. (56). The corrected fluorescence intensity, F', is given by

$$F' = \beta_1 \beta_2 F ,$$

where β_1 and β_2 are the constants defined on page 55 .

Plots of F' against $TlBr_2^-$ concentration were made for a series of solutions at z = 0.5, 1.0, 2.0, 3.0, and 4.0 M, for 470 mμ emission and excitation at 240, 250, 260, and 270 mμ excitation. Presented in Figure 18 are representative plots. Similar plots were prepared for emission at 410, 440, and 500 mμ with 250 mμ and 260 mμ excitation.

Corresponding to each value of z is a slope which is equal to

$$\text{slope} = \beta_1 \beta_2 \left[\frac{z^2}{K_{4_c}} y_4 + y_2 + \frac{K_2}{z} y_1 + \frac{K_1 K_2}{z^2 f_{\pm}^2} y_0\right] .$$

The linear equations, corresponding to each value of z, were solved simultaneously to obtain the y value for each species. The values of

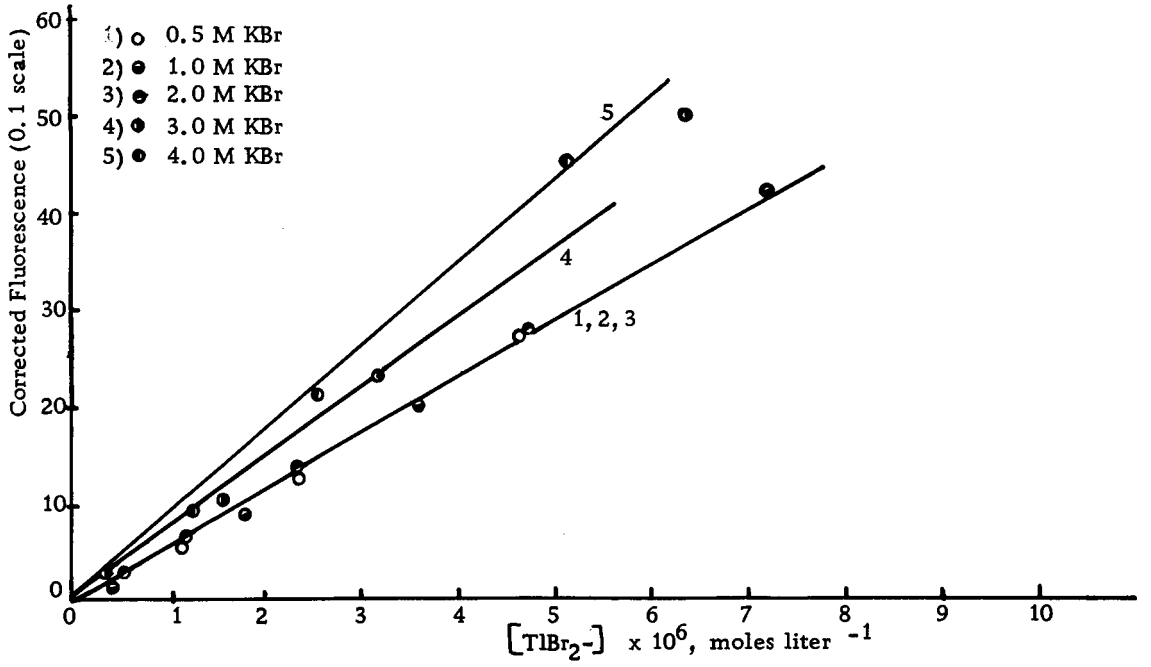

260 mu Excitation, 470 mu Emission

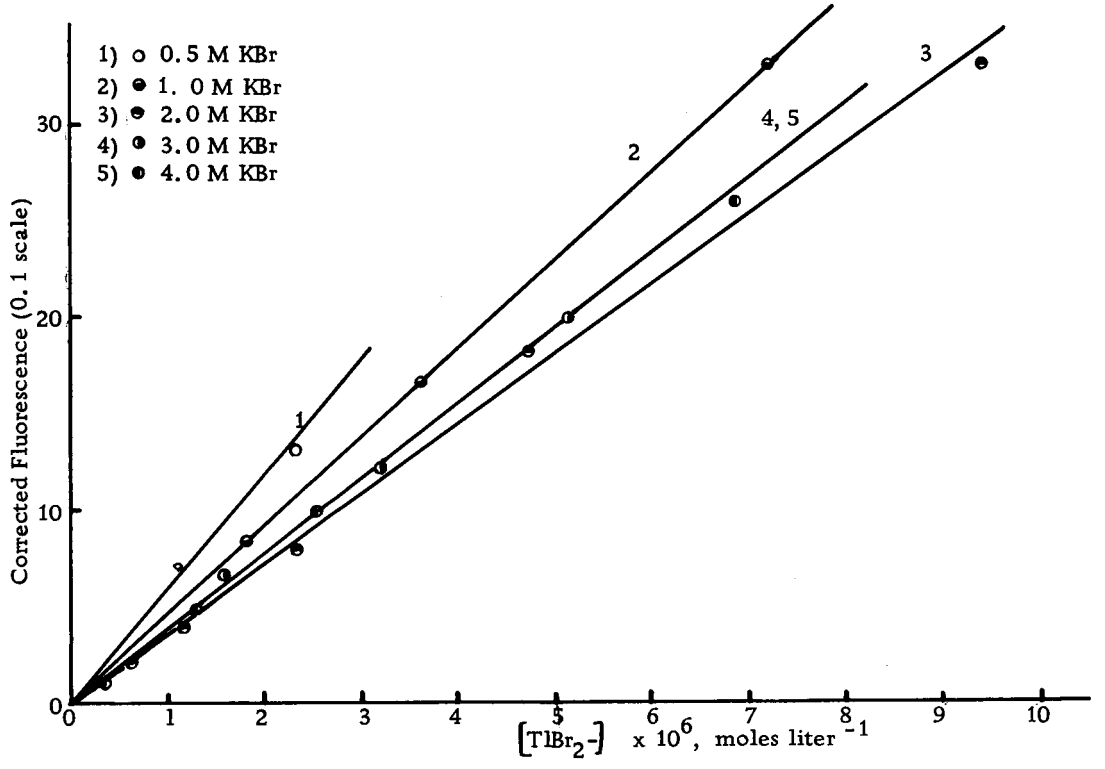

260 mu Excitation, 470 mu Emission

Figure 18. Variation of emission intensity with $TlBr_2^-$ concentration

$\beta_1 \beta_2 y_n$ obtained by this method are summarized in Table 12.

Table 12. $\beta_1 \beta_2 y_n$ values calculated from F' vs $TlBr_2^-$ concentration plots

a) 470 mμ Emission

Excitation wavelength, mμ	Tl^+	TlBr	$TlBr_2^-$	$TlBr_4^{\equiv}$
240	0	4.2×10^6	3.3×10^6	2.4×10^5
250	0	1.7×10^6	6.0×10^6	2.7×10^5
260	0	0	6.0×10^6	2.6×10^6
270	0	0	2.6×10^6	3.3×10^6

b) 250 mμ Excitation

Emission wavelength, mμ	Tl^+	TlBr	$TlBr_2^-$	$TlBr_4^{\equiv}$
410	0	1.6×10^6	1.1×10^6	0
440	0	2.0×10^6	3.9×10^6	1.8×10^5
470	0	1.7×10^6	6.0×10^6	2.7×10^5
500	0	1.2×10^6	5.4×10^6	7.2×10^5

c) 260 mμ Excitation

Emission wavelength, mμ	Tl^+	TlBr	$TlBr_2^-$	$TlBr_4^{\equiv}$
410	0	0	1.2×10^6	4.5×10^5
440	0	0	3.6×10^6	2.1×10^6
470	0	0	6.0×10^6	2.6×10^6
500	0	0	4.8×10^6	3.3×10^6

Since $y_n = I x O_n \epsilon_n$ and I, x, β_1, β_2 are constants, the ratio $\beta_1 \beta_2 y_n / \epsilon_n$ is proportional to the quantum yield, ϕ_n. These ratios were plotted against the emission wavelength. By drawing symmetric curves through the points, the approximate wavelength of the emission maximum for each species may be ascertained.

The variation of $\beta_1 \beta_2 y_n/\epsilon_n$ with emission wavelength is shown in Figure 19. The emission maximum is located at 440 mμ for TlBr, 475 mμ for $TlBr_2^-$, and 495 mμ for $TlBr_4^{\equiv}$. Though Tl^+ is not presented in Figure 19, the emission maximum is located at 360-370 mμ. It is also evident from Figure 19 that the quantum yield is greatest for TlBr and least for $TlBr_4^{\equiv}$. A comparison of Figure 17 and Figure 19 shows a reversal of order. The reason for this reversal is unknown.

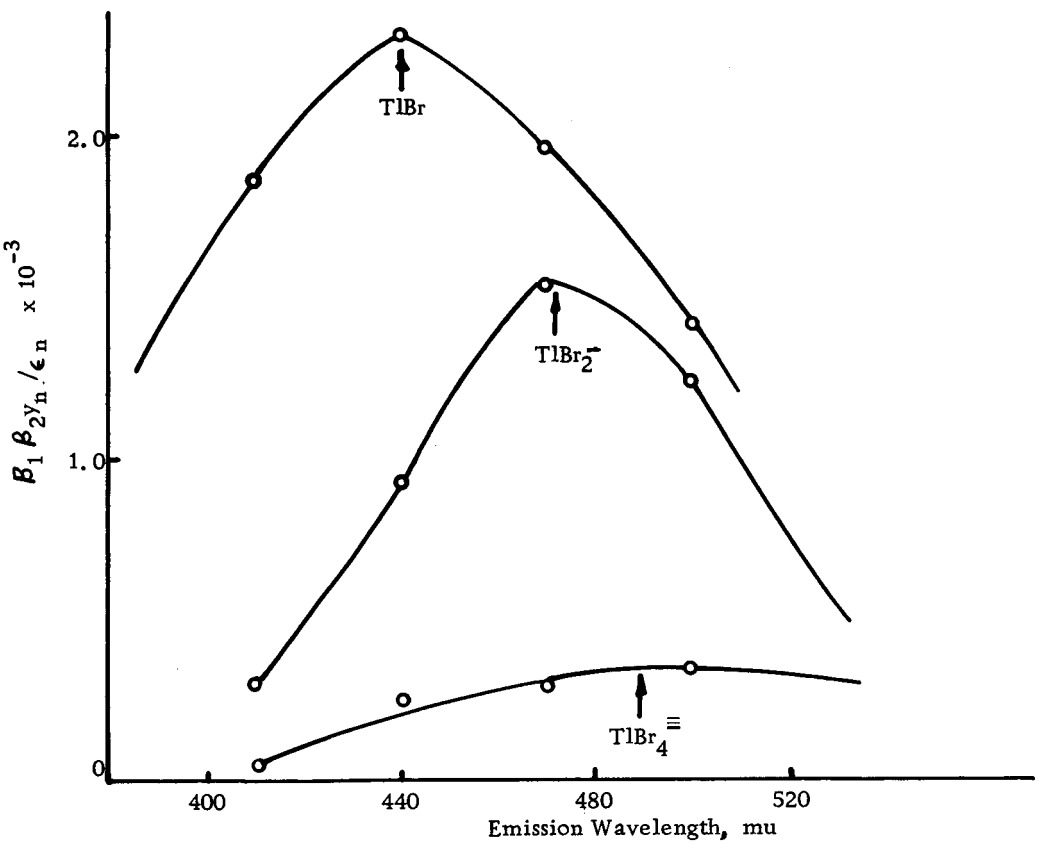

Figure 19. Variation of $\beta_1 \beta_2 y_n/\epsilon_n$ with emission wavelength for KBr:TlBr solutions

The values of $\beta_1 \beta_2 y_n$ were used in conjunction with the concentration of each species present in KBr:TlBr solution to calculate the percentage of the fluorescence which is due to each species. The calculated percentages are given in Table 13.

Table 13. Percent fluorescence due species present in KBr:TlBr solutions
470 mμ Emission

KBr Conc., m/l	% Fluorescence due to	Excitation Wavelength, mμ 240	250	260	270
0.5	TlBr	43	23	0	0
	$TlBr_2^-$	57	77	100	100
1.0	TlBr	28	13	0	0
	$TlBr_2^-$	72	87	100	100
2.0	TlBr	7	5	0	0
	$TlBr_2^-$	93	95	100	100
3.0	TlBr	4	3	0	0
	$TlBr_2^-$	87	87	80	80
	$TlBr_4^{\equiv}$	9	10	20	20
4.0	TlBr	3	2	0	0
	$TlBr_2^-$	82	80	70	60
	$TlBr_4^{\equiv}$	15	18	30	40

Due to the lack of reliable absorption and emission data for KI:TlI solutions, no attempt was made to analyze the weakly fluorescent spectra of KI:TlI solutions.

The error involved in the analysis of the emission spectra of KCl:TlCl and KBr:TlBr solutions by the method outlined in this section is estimated to be 15 percent.

D. Fluorescence Quantum Yields

In order to obtain absolute quantum yields, it is necessary to know the number of quanta absorbed and the number emitted. Since the fluorescence radiation was too weak to be detected by the thermopile-galvanometer system, the activation of a photographic emulsion by the fluorescence radiation was used to measure the fluorescence energy.

The film calibration curve in which the optical density of the silver deposit on the developed film was plotted against the logarithm of the exposure is given in Figure 20. The exposure is defined as the product of the radiant flux density of the standard lamp and the time that the film was exposed to this radiant flux. Since Kodak Panatomic-X film is responsive only to radiation in the spectral region 360 mμ to 660 mμ, the film will detect approximately 4.5 percent of the total radiation emitted by a blackbody at 2800^{o}K (14). This was taken into account in the calculation of the exposure, the logarithm of which was used in Figure 20.

The exposure corresponding to the optical density of the film which had been exposed to the fluorescing solution was obtained from the film calibration curve. Presented in Table 14 are the results for KCl:TlCl solutions.

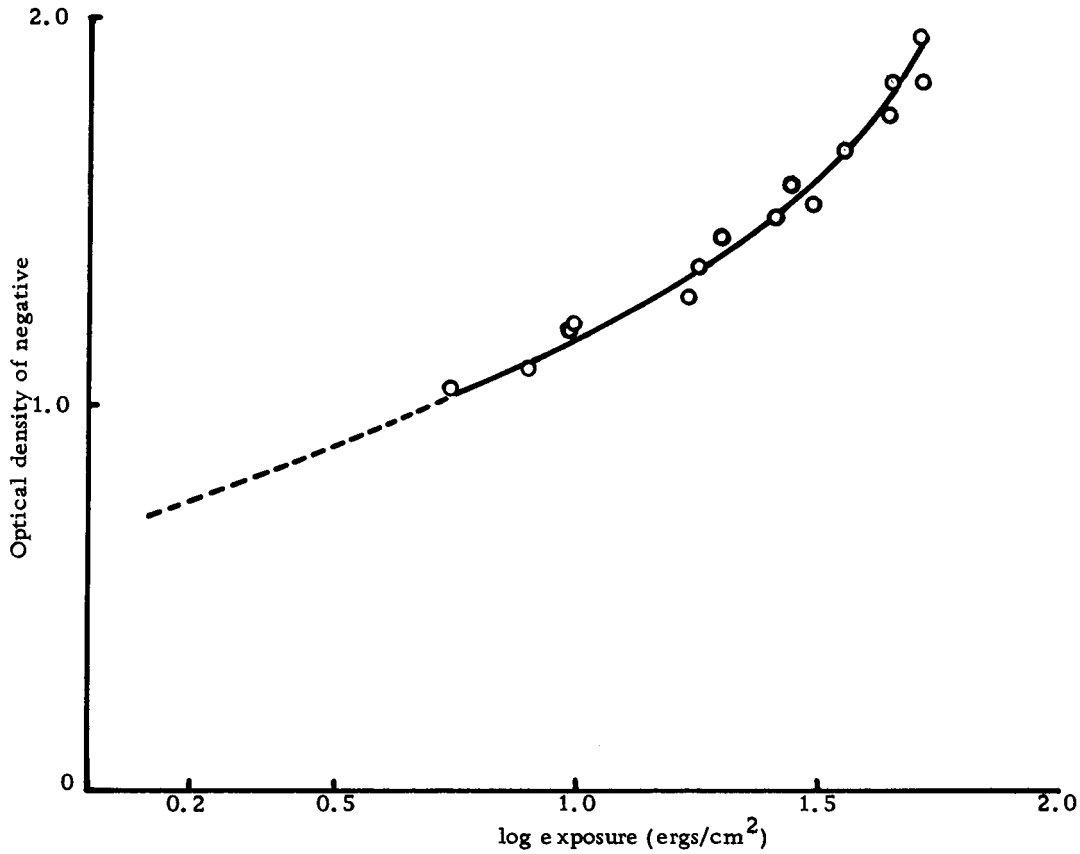

Figure 20. Kodak Panatomic-X Film calibration curve

Table 14. Results of the photographic determination of the radiant flux from KCl solutions containing 2.67×10^{-4} M TlCl. Excitation at 250 mμ

KCl Conc., mole/liter	Exposure time, sec.	Exposure obtained from Figure 20, ergs cm^{-2}	Radiant flux density, ergs cm^{-2}sec^{-1}
4.0	60.4	5.6	9.3×10^{-2}
4.0	120.4	10.8	9.0×10^{-2}
3.0	75.3	5.3	7.0×10^{-2}
3.0	135.6	7.6	5.6×10^{-2}
2.0	90.2	(3.5)	(3.9×10^{-2})
2.0	180.8	(4.5)	(2.5×10^{-2})

Values in brackets were obtained from the extrapolated portion of Figure 20.

Since the film was positioned 9.3 cm from the center of the fluorescence radiation, the total fluorescence energy, E_F, is given by the product of the radiant flux density (Table 14) and the area of a sphere with a radius of 9.3 cm. The energy absorbed, E_A, at 250 mμ was calculated from the absorbance of the solution and the intensity of exciting radiation, calculated from the data of Figure 7. The efficiency, e_F, of the fluorescence process will be defined by

$$e_F = \frac{E_F}{E_A} .$$

Finally, since the fluorescence maximum for KCl:TlCl solutions is located at 440 mμ and since the energy of a photon at 250 mμ is equivalent to the energy of 1.760 photons at 440 mμ, an estimate of the fluorescence quantum yield may be obtained from the product $1.760\ e_F$. For the KCl:TlCl solutions given in Table 14, e_F is 0.056, 0.095, and 0.123 and the quantum yield is 0.100, 0.167, and 0.217 for 2.0, 3.0, and 4.0 M KCl respectively. Since the actual filament temperature of the standard lamp is not known and was assumed to be 2800°K, these quantum yields are rough estimates only.

Morgenshtern (42) has investigated the absolute quantum yield of photoluminescence of single crystal alkali halide:thallium phosphors. For a KCl phosphor containing 1.5×10^{-4} g of Tl per g

of KCl, Morgenshtern reported a quantum yield of 0.80 (246 mμ excitation).

E. KNO_3 containing TlCl

The basis of the Seitz-Williams model of the luminescence center for KCl:Tl single crystal phosphors is that the absorption and emission spectra are due to electronic transitions within the thallous ion. If KNO_3 were used instead of KCl, a similar absorption and emission spectrum should be observed for the thallium-containing salt. Experimentally, it was observed that the thallium-containing KNO_3 salt is not luminescent. Makishima and coworkers (39), however, have found that single crystal phosphors of $NaNO_2$:Tl are luminescent with an emission band in the blue region of the spectrum which they attribute to the nitrite ion and another band in the red region of spectrum which is attributed to the thallous ion.

IV. DISCUSSION AND CONCLUSIONS

A. Introduction

In order to discuss complex ion formation, the stability of complex species, and the interpretation of absorption and emission spectra of complexes, it is necessary to consider the variables associated with the central thallous ion, the halide ligands, and the solvent. Assembled in Table 15 are most of the parameters that will be used in discussing these problems. Wherever reference is made to an ion, the singly charged ion is inferred.

Table 15. Atomic and Ionic Constants (11, 34)

Element	K	Tl	F	Cl	Br	I
Ionic Radius, Å	1.33	1.51	1.36	1.81	1.96	2.19
Ionization Potential, ev	4.34	6.10	17.41	13.01	11.84	10.44
Electron Affinity, ev	---	---	3.62	3.78	3.54	3.28
Electronegativity	0.91	1.44	4.10	2.83	2.74	2.21
Polarizability of ion x 10^{24}, cm^{-3}	1.00	3.90	0.81	2.98	4.24	6.45
Hydration enthalpy of ion, kcal/mole*	-75.0	-76.2	-122	-89.8	-81.7	-71.3
Hydration entropy of ion, e.u.*	-17.03	-16.03	-32.3	-18.8	-15.1	-9.6

* at 25°C

B. Complex formation and the stability of thallous halides

Thallium (I) has a valence electron configuration $6s^2$, a ^1S_o ground state. The thallous ion shows little tendency to form fluoro-, cyano-, or hydroxo-complexes; however, it does form chloro-, bromo-, iodo-, and thiocyanato-complexes. The solubility of the monovalent thallium halides decreases as the polarizability of the halide ion increases, therefore TlF is the most soluble and TlI the least soluble. In terms of Pauling's criterion of electronegativity differences as a measure of the percent ionic character of a single bond, the solubilities of the thallous halides parallel the percent ionic character of the single bond, thus TlF has approximately 82% ionic character and TlI approximately 12%.

The formation of complexes has received much theoretical work in the past decade. The main theoretical approaches which have been used to discuss complex formation are 1) the valence bond method due to Pauling, 2) the molecular orbital method, 3) the Bethe-Schlapp-Penney crystal field theory, and 4) the VanVleck-Mulliken ligand field theory.

The most direct and most easily visualized method is that due to Pauling. In this method, orbitals of the central atom are made available for the formation of covalent bonds. Using the criterion of maximum overlap, sigma bonds are formed when the vacant metal orbital and the filled orbital of the donor group, the ligand, occupy the same space; that is, the overlap integral is a

maximum. In the case of the thallous ion, the vacant metal orbitals are the 6p and 7s (the 6d and 5f are also available). The halide ligands may then form linear TlX_2^-, trigonal $TlX_3^{=}$, tetrahedral $TlX_4^{\equiv}$, or octahedral TlX_6^{-5} by donating electron pairs for the formation of coordinate covalent bonds with the thallous ion.

While Pauling's method is useful qualitatively, the quantitative consideration of bond energies, of the stability of complexes, of observed energy levels, and absorption and emission spectra often cannot be ascertained by this method.

One of the approaches that will be used in the discussion presented here for the formation of complexes is electrostatic in nature. First, the energy of formation of complexes from the gaseous ions, in vacuo, will be calculated.

If varying numbers of halide ions of radius r_- are added to the positively-charged, spherically-symmetrical thallous ion of radius r_+, then using Coulomb's law, the energy which is released will be given by

$$U_1 = \frac{-ae^2}{(r_+ + r_-)_e} + \frac{be^2}{(r_+ + r_-)_e} \quad ,$$

where a and b are constants dependent upon the number of halide ions added and the geometrical arrangement of these ions and the subscript e refers to the equilibrium internuclear distance. The halide ions will be arranged geometrically such that their mutual repulsion, i.e. the second term in the above expression, is

minimal. As examples, for linear TlX_2^- complexes the energy equation will be given by:

$$U_1 = \frac{-2e^2}{(r_+ + r_-)_e} + \frac{e^2}{2(r_+ + r_-)_e} \quad ,$$

for trigonal $TlX_3^=$ complexes

$$U_1 = \frac{-3e^2}{(r_+ + r_-)_e} + \frac{3e^2}{(r_+ + r_-)_e\sqrt{3}} \quad ,$$

and for tetrahedral $TlX_4^{\equiv}$ complexes

$$U_1 = \frac{-4e^2}{(r_+ + r_-)_e} + \frac{6e^2}{1.633(r_+ + r_-)_e} \quad .$$

Since the halide ions are polarizable, calculations of the formation energy necessitate the inclusion of a term for the interaction energy between the thallous ion and the dipole moment induced by the field of the thallous ion. The interaction energy, U_2, is given by

$$U_2 = \frac{-1}{2} \frac{\alpha e^2}{(r_+ + r_-)_e 4} \quad ,$$

where α is the polarizability of the halide ion.

Finally, due to the fact that the thallous ion is itself polarizable, an attractive energy results from London-Van der Waals interaction. This energy, called the London dispersion energy and denoted by U_3, may be written as

$$U_3 = \frac{-3}{2} \frac{\alpha_+ \alpha_-}{(r_+ + r_-)_e 6} \frac{I_+ I_-}{I_+ + I_-} \quad ,$$

where I is the ionization potential.

The total energy released in the formation of an ion-ion complex is equal sum of the Coulombic law energy, the ion-induced dipole energy, and the London dispersion energy; i.e.

$$U_{total} = U_1' + U_2 + U_3 \quad .$$

Listed in Table 16 are the calculated values for U_1', U_2, U_3 and U_{total}. These calculations were made assuming anion-cation contact and linear, trigonal, and tetrahedral configurations for TlX_2^-, $TlX_3^=$, and $TlX_4^{\equiv}$ respectively. In order to correct U_1 for the repulsion energy, the calculated values of U_1 were corrected by subtracting 19.5, 19.2, and 18.8 percent of the calculated U_1 value for chloride, bromide, and iodide complexes respectively. These percentage values were obtained from the repulsion energies calculated (34, p. 43) for the thallous halide crystals by the method of Born. The corrected values of U_1 are denoted by U_1' in Table 16.

Also listed in Table 16 are the dissociation constants for the complexes. The parallel between the stability of the complex and the electrostatic energy of formation of the complex is reflected in that the dissociation constant increases with decreasing $-U_{total}$ for a given halide. The parallel also exists for $TlX_4^{\equiv}$ complexes; however it is reversed for TlX_2^- complexes. It is evident from the table that only qualitative comparisons are valid.

Table 16. U_1', U_2, U_3, and U_{total} for TlX complexes

Complex	$-U_1'$	$-U_2$	$-U_3$	$-U_{total}$	Dissociation Constant
	kcal/mole				
$TlCl_2^-$	121.43	8.14	2.50	132.07	1.87
$TlCl_4^{\equiv}$	26.00	16.28	5.00	47.28	93
$TlBr_2^-$	116.05	9.61	2.62	128.28	0.30
$TlBr_4^{\equiv}$	25.04	19.22	5.24	49.50	16
TlI_2^-	109.39	11.44	2.62	123.45	0.26
$TlI_3^=$	92.55	17.16	3.93	113.64	2.0
$TlI_4^{\equiv}$	23.58	22.88	5.24	51.70	3.5

The foregoing calculation does not take into consideration two important features of complex ion formation in a solvent. First, if the solvent is water, the interaction energy should be much less because of the high dielectric constant, D_{H_2O}, of the medium. It is uncertain what constant to use in computations of this kind; dividing by D_{H_2O} will give a lower limit to the energy. Second, a more realistic approach is to consider that the complexes are formed by reactions between hydrated ions and that the complex formation may be considered as the replacement of a water ligand in the coordination sphere of thallium (I) by a halide ligand.

C. Thermodynamics of Coordinate Bond Formation

With the aid of experimental dissociation constants and consideration of the reactions in solution, it is possible to calculate metal-halide single bond energies. Consider that the reactions in solution, together with the corresponding enthalpy changes, may be represented as follows:

$$Tl(H_2O)_n^{+1} + X^-_{(aq)} = \left[Tl(H_2O)_{n-1}X\right] + xH_2O\ ;\Delta H_1 \quad (1)$$

$$\left[Tl(H_2O)_{n-1}X\right] + X^-_{(aq)} = \left[Tl(H_2O)_{n-2}X_2\right]^- + xH_2O\ ;\ \Delta H_2 \quad (2)$$

$$\left[Tl(H_2O)_{n-2}X_2\right]^- + 2X^-_{(aq)} = \left[Tl(H_2O)_{n-4}X_4\right]^{\equiv} + xH_2O;\ \Delta H_4 \quad (4)$$

In the above, ΔH gives the energy (strictly speaking the enthalpy) required to break a Tl-H_2O bond and form a Tl-X bond, provided the energy for removal of X from its hydration sphere is neglected. Estimates of the stepwise enthalpy changes can be made from the successive formation constants K_1', K_2'', etc., which are the inverse of the experimentally determined dissociation constants, and the entropy change for the reaction. The standard free energy ΔF° for a reaction is given by the relation

$$\Delta F^\circ_n = -2.303\,RT \log K_n' \ .$$

The enthalpy is related to ΔF°_n by the expression

$$\Delta H^\circ_n = \Delta F^\circ_n + T\,\Delta S^\circ_n \ .$$

The entropy change ΔS_1^o for reaction (1) may be obtained by considering the following processes together with corresponding entropy changes:

$$Tl^+ (g) + X^- (g) = TlX (g) \; ; \; \Delta S^o_{TlX}$$

$$Tl^+ (H_2O)_n^{+1} = Tl^+ (g) + n\, H_2O \; ; -\Delta S^o_{Tl^+ \text{ hydration}}$$

$$X^- (H_2O)_n^{+1} = X^- (g) + n\, H_2O \; ; -\Delta S^o_{Cl^- \text{ hydration}}$$

$$TlX (g) + n\, H_2O = TlX (H_2O)_n \; ; \; \Delta S^o_{TlCl \text{ hydration}}$$

The sum of the four equations will give the desired overall equation; therefore,

$$\Delta S_1^o = \Delta S^o_{TlX} - \Delta S^o_{Tl^+ \text{ hydration}} - \Delta S^o_{X^- \text{ hydration}} + \Delta S^o_{TlX \text{ hydration}}$$

The standard entropies and entropy changes at 25°C, which were used to calculate ΔS_1^o, are presented in Table 17.

Table 17. Standard entropy and hydration entropy at 25°C in cal/deg/mole

	S^o (g), e.u.	$\Delta S^o_{\text{hydration}}$, e.u.
Tl^+	41.9[a]	-16.03[b]
Cl^-	36.3[a]	-18.85[b]
Br^-	39.2[a]	-15.13[b]
I^-	40.6[a]	- 9.63[b]
TlCl	61.1[a]	-19.0 [c]
TlBr	63.8[a]	-17.3 [c]
TlI	65.6[a]	-16.2 [c]

a (52) , b (34, p. 105) , c (43)

Presented in Table 18 are the calculated thermodynamic quantities for reaction (1).

Table 18. Thermodynamic values for the formation reaction of $\left[Tl(H_2O)_{n-1}\ X\right]$ complexes

Complex	Formation constant (observed)	ΔS_1°, e.u.	Calculated ΔF_1°, kcal/mole	ΔH_1°, kcal/mole
$\left[Tl(H_2O)_{n-1}\ Cl\right]$	4.00	-1.07	-0.82	-1.14
$\left[Tl(H_2O)_{n-1}\ Br\right]$	4.16	-3.44	-0.84	-1.86
$\left[Tl(H_2O)_{n-1}\ I\right]$	29.41	-7.44	-2.00	-4.22

No attempt was made to calculate the thermodynamic quantities for the formation reactions of $\left[Tl(H_2O)_{n-2}\ X_2\ \right]^-$ or $\left[Tl(H_2O)_{n-4}\ X_4\right]^{\equiv}$. The reason for this was the lack of hydration entropy values for these complexes.

In order to obtain metal-halide single bond energies, it is necessary to know the metal-water molecule bond energy and ΔH_1° (Table 18). An estimate of the metal-water molecule bond energy can be calculated from the experiment hydration enthalpy and the coordination number, n, of the thallous ion. While there is no method known for the unambiguous determination of n, its estimation from a realistic structural model is possible.

The coordination number of the thallous ion may be obtained by considering the structure of water. The structure of water in the immediate neighborhood of the Tl^+ ion was assumed to be similar to that of ice. In the ice structure, which is shown in Figure 21a,

each oxygen atom is surrounded tetrahedrally by four other oxygen atoms at a distance of 2.76 Å. Presented in Figure 21b is a portion of the ice structure with a Tl^+ ion located in the body center of the unit; therefore, the Tl^+ ion has eight nearest neighbor water molecules and its coordination number is eight.

Figure 21. Structure of ice

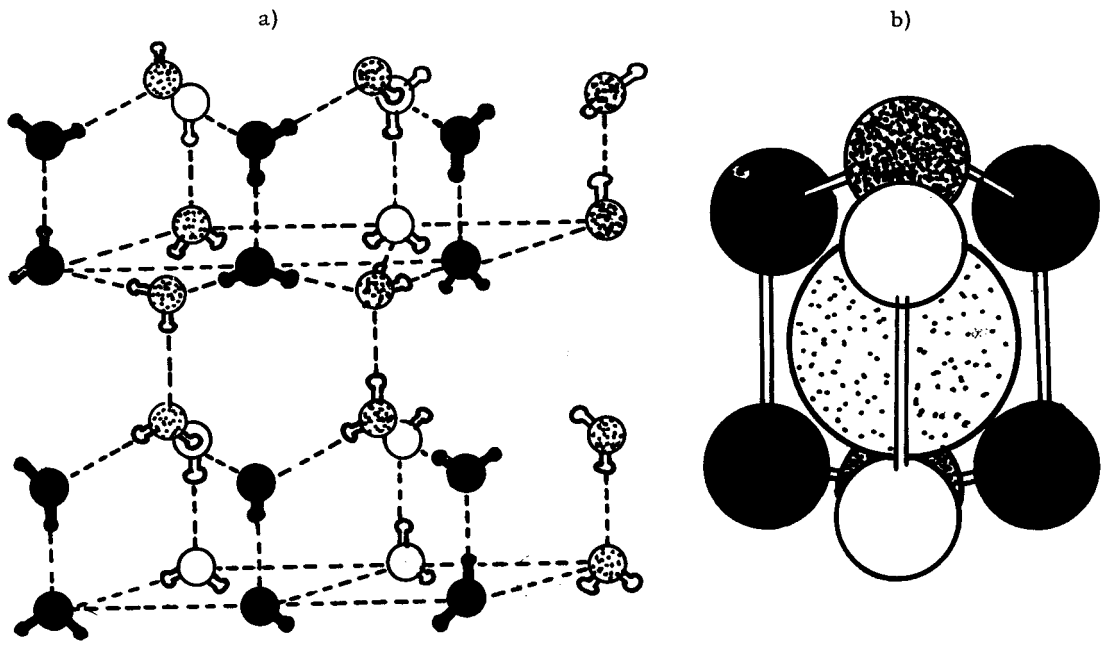

a) Arrangement of molecules in the ice structure (46)

b) Ice structure with a thallium (I) ion in the body center

Since the experimental hydration enthalpy is -76.2 kcal/mole for Tl^+ (Table 15) and the coordination number is eight, the thallium-water molecule bond energy is -9.5 kcal/mole. The enthalpy of formation (Table 18) determines the difference in bond energy between that of the coordinated water molecule and that of the

coordinated halide; therefore, the thallium-halide single bond energy is -10.6, -11.4, and -13.7 kcal/mole for Tl-Cl, Tl-Br, and Tl-I respectively. These values for the thallium-halide single bond energies are in accord with the order of the observed dissociation constants for TlCl (0.26), TlBr (0.24), and TlI (0.034).

The electrostatic part of the metal-ligand bond energy may be calculated from the Born equation which gives the electrostatic part of the enthalpy of hydration. The Born equation for the hydration enthalpy is given by (35, p. 123)

$$\Delta H^{o}_{Born} = -\frac{1}{2}\frac{Ne^2}{r}\left(1 - \frac{1}{D} - \frac{T}{D^2}\frac{dD}{dT}\right) ,$$

where N is Avogadro's number, D is the dielectric constant of water at temperature T, and r is the radius of the central ion plus 2.76 Å, the diameter of a water molecule. At 25°C, the dielectric constant of water is 78.54 and dD/dT is 0.3613. For the hydrated thallous ion, the hydration enthalpy calculated from the Born equation is -37.7 kcal/mole; therefore, the electrostatic part of the thallium-water molecule bond energy is -4.7 kcal/mole.

D. Interpretation of absorption and emission spectra

1. Single crystal phosphors. The emission and absorption spectra of single crystal KCl:Tl phosphors have been interpreted by Williams et al. (26-29, 66-68) as transitions between the ^1S_o ground state of Tl^+ and the excited 6s6p states consisting of the triplet state $^3P_{o,1,2}$ and the singlet state $^1P_1$. The 196 mμ absorption and the 475 mμ

emission are ascribed to $^1S_o \longleftrightarrow {}^1P_1$ transitions and the 247 mμ absorption and 305 mμ emission to $^1S_o \longleftrightarrow {}^3P_1$ transitions.

2. Electron transfer spectra. The similarity between the absorption spectrum of KCl:Tl and KBr:Tl single crystal phosphors with that of the corresponding aqueous solution was shown in Figure 1. The spectra of aqueous thallous halide complexes may be interpreted as electron transfer spectra. Electron transfer transitions occur in complexes formed between electron donors and electron acceptors and give rise to intense absorption bands not found in either the acceptor or donor (5, 13, 30). Mulliken (40) refers to these as charge-transfer transitions.

Since electron transfer is an oxidation-reduction process, a qualitative description of the absorption bands may be related to the oxidizing strength of the central ion and the reducing strength of the ligand. For the thallous halide complexes, the shift of the absorption maximum towards longer wavelengths with increasing atomic number of the halide is consistent with the reducing power of the halide ions, $Cl^- < Br^- < I^-$; for example, the absorption maximum is at 223 mμ for TlCl, 243 mμ for TlBr, and 280-300 mμ for TlI.

The mechanism in many cases is regarded as the transfer of an electron from the ligand to the central metal ion, thereby decreasing the oxidation number of the cation by one. Various authors have described other mechanisms to account for the electron transfer transitions. Among those that have been proposed are electron

transfer from the cation or anion to the solvent and electron transfer from an anion not in the coordination sphere to the complex. The latter mechanism has been used for cationic complexes having highly polarizable anions nearby. For example, $Co(NH_3)_6^{+3}$ with the iodide ion forms the excited state $Co(NH_3)_6I^{+2}$ thus forming an ion-pair (13).

Katzin (32) has assembled a large mass of data on the absorption spectra of halides. He concludes that the electron transfer bands are due to transfer of electrons localized on the halide portion of the molecule or ion, leaving the neutral halogen atom, either in the $^2P_{3/2}$ ground state or the $^2P_{1/2}$ excited state, as part of the excited state configuration. The assignment of a given portion of the absorption spectrum to the halide component was made on the basis of the halogen atom spectrum, which has a pair of levels, $^2P_{3/2}$ - $^2P_{1/2}$, with a characteristic spacing of 7600 cm^{-1} for iodine, 3700 cm^{-1} for bromine, and 800 cm^{-1} for chlorine. Katzin presumes that whenever a bromide or iodide exhibits a pair of peaks with approximately the required spacing, then the absorption of that part of compound is being observed. Since the characteristic separation of the pair of levels for chloride is too small to be resolved by most instruments, single peaks are generally observed for chlorides. Katzin does not attempt to identify the mechanism of the electron transfer, that is, whether the electron is transferred to the metal or to the solvent.

If the electron transfer is considered to be from the ligand to the central metal, then for TlX complexes, the following Born-Haber cycle will be considered:

$$\begin{array}{ccc} TlX & \xleftarrow{-\Delta H_{coulombic}} & Tl^{+} + X^{-} \\ \downarrow \Delta H_{transition} & & \uparrow I - E.A. \\ Tl^{o}X^{o} & \xrightarrow[W]{} & Tl^{o}(g) + X^{o}(g) \end{array}$$

For the cycle,

$$\Delta H_{transition} + W + (I\text{-}E.A.) + (-\Delta H_{coulombic}) = 0 .$$

The energy (strictly speaking the enthalpy) of the transition is related to the transition wavelength, λ , by

$$\Delta E_{transition} = \frac{hc}{\lambda_{transition}} .$$

Therefore,

$$\frac{hc}{\lambda_{transition}} = E.A. - I - W + \Delta H_{coulombic} ,$$

where I is the ionization potential of the metal, E.A. is the electron affinity of the ligand, W is the dissociation energy of the excited state, and ΔH is the coulombic potential. For TlX_2^- complexes the dissociation of the excited state is given by

$$\left[X\,Tl^{o}X^{o}\right]^{-} \xrightarrow{W} \left[X\,Tl^{o}\right]^{-} + X^{o} ,$$

and for $TlX_4^{\equiv}$ complexes by

$$\left[\begin{array}{c} X \\ X\ Tl^{o}X^{o} \\ X \end{array}\right]^{\equiv} \xrightarrow{W} \left[\begin{array}{c} X \\ X\ Tl^{o} \\ X \end{array}\right]^{\equiv} + X^{o} .$$

The dissociation energies of the electron transfer excited state of the thallous halide complexes were calculated using the ionization potentials and electron affinities given in Table 15 and the wavelength of the absorption maximum for each complex. These dissociation energies are presented in Table 19.

Table 19. Dissociation energy of the electron transfer excited state for thallous chloride and thallous bromide complexes

Complex	Absorption maximum, mμ (observed)	-W, e.v. (calculated)
TlCl	223	3.53
$TlCl_2^-$	243	3.07
$TlCl_4^{\equiv}$	254	2.85
TlBr	243	3.42
$TlBr_2^-$	252	3.30
$TlBr_4^{\equiv}$	266	3.04

It is clear that, since I and E.A. are constant among the chloride or bromide complexes, the shift of the absorption maximum to longer wavelengths with increasing coordination number is due to a decrease in W.

3. Oscillator strengths of the electron transfer transitions . In order to determine the oscillator strength f of the electron transfer transitions, the molar extinction coefficients for each thallous-halide complex were plotted as a function of the frequency, ν, in

cm^{-1}. The oscillator strength is related to the area under the curve by (4, p. 81)

$$f = 4.32 \times 10^{-9} \int \epsilon \, d\nu \quad ,$$

where $\int \epsilon \, d\nu$ is the area in liter $mole^{-1}$ cm^{-2}. The areas and the oscillator strengths are given in Table 20.

Two other parameters of interest may be calculated from the oscillator strength and the frequency of the absorption maximum. These quantities are $t_{1/2}$, the time required for the number of molecules in the excited state to decrease by one-half, and L, an estimate of the distance the electron moves in the electron transfer process. According to Barrow (4, p. 310) $t_{1/2}$ is expressed by the following equation

$$t_{1/2} = \frac{0.55 \times 10^{9}}{(\nu)^{2} f} \quad ,$$

where ν is the frequency of the absorption maximum in cm^{-1}. The equation for L (33, p. 688) is

$$L = \sqrt{\frac{f\lambda}{1080}} \quad ,$$

where λ is the wavelength of the absorption maximum in angstroms. Values of $t_{1/2}$ and L are presented in Table 20. The values of $t_{1/2}$, approximately 10^{-8} seconds, are in accord with Pringsheim's estimate of the lifetime of the fluorescence excited state. The values of L, all of which are approximately 0.5 Å, do not give an indication as to whether the electron transfer is to a solvent molecule or to the central metal.

Table 20. Oscillator strength, $t_{1/2}$, and L for thallous halide complexes

Complex	$\int \epsilon \, d\nu$ liter mole^{-1}cm^{-2}	f	$t_{1/2}$, sec	L, Å
TlCl	1.96×10^{7}	0.085	1.43×10^{-8}	0.42
$TlCl_2^-$	2.16×10^{7}	0.093	1.51×10^{-8}	0.46
$TlCl_4^{\equiv}$	2.13×10^{7}	0.092	1.67×10^{-8}	0.46
TlBr	1.93×10^{7}	0.084	1.71×10^{-8}	0.43
$TlBr_2^-$	2.24×10^{7}	0.097	1.58×10^{-8}	0.48
$TlBr_4^{\equiv}$	3.91×10^{7}	0.169	1.01×10^{-8}	0.65

Since the oscillator strengths listed in Table 20 are approximately 0.1, it would appear that the electron transfer transitions are those normally referred to as "allowed". Jorgensen (30) has suggested that four types of electron transfer are to expected if relatively pure molecular orbital configuration are assumed. Two of the four types, namely $\pi \longrightarrow$ even γ_5 and $\sigma \longrightarrow$ even γ_3, are "allowed" transitions. In tetrahedral symmetry, the orbitals of the central ion are γ_5 for p-electrons and γ_3 and γ_5 for d-electrons. Thus considering the thallous ion electron configuration, the most likely electron transfer transition for thallous halide tetrahedral complexes is $\pi \longrightarrow$ even γ_5.

The very intense absorption bands characteristic of the thallous iodide complexes indicate that their oscillator strengths will be larger than those of the thallous chloride and thallous bromide complexes. This is in agreement with Dunn's (13) observation

that the relative intensities of electron transfer bands are proportional to the Lande' multiplet splitting factor, which is 587 cm^{-1} for Cl, 2457 cm^{-1} for Br, and 5069 cm^{-1} for I.

4. Comparison of single crystal phosphors with solutions of the same composition. The close parallel between the absorption and emission spectra of thallium (I)-alkali halide crystal phosphors and that of the thallous halide complexes in solution is illustrated in Table 21.

Table 21. Absorption and emission peaks ($m\mu$)

	Phosphors		Solutions	
	Absorption Maxima	Emission Maxima	Absorption Maximum	Emission Maximum
KCl:TlCl	196 247	305 470	243	430
KBr:TlBr	210 262	318 430-500	263	470
KI:TlI	236 287	415	300	530-550

The similarity of the absorption and emission spectra suggests that the spectra of the single crystals phosphors are due to complex aggregates within the crystal lattice and that treatment by electron transfer theory would be worthwhile.

E. Quenching of the fluorescence

Even though the thallous iodide complexes exhibit strong absorption bands, their fluorescence intensity is approximately 0.0002 that of the thallous chloride complexes and approximately 0.0006 that of thallous bromide complexes with the same total thallium and halide concentration. The low fluorescence yield of thallous halide complexes may be caused by photochemically active species in the electron transfer excited state. An alternate explanation is that quenching occurs. In equation form, the process of excitation and emission may be written as follows:

$$\left[Tl X_n\right] + h\nu \longrightarrow \left[Tl X_n\right]^* \quad \text{excitation}$$

$$\left[Tl X_n\right]^* \longrightarrow \left[Tl X_n\right] + h\nu' + E \quad \text{emission}$$

where * denotes an excited state and E is energy; the frequency ν is greater than ν'. If quenching takes place, the quenching reaction is

$$\left[Tl X_n\right]^* + X \longrightarrow \left[Tl X_n X\right]^* \longrightarrow \text{products} + E \cdot$$

Numerous studies (47) have shown that the iodide ion is a very efficient quencher, thus the low fluorescence yield of thallous iodide complexes may very well be due to the quenching action of the iodide ion. (Quenching, due to the halide ion, is also noticeable in concentrated KCl:TlCl and KBr:TlBr solutions.)

V. SUMMARY

1. Evidence is given that in KCl solutions of concentration greater than 2.5 M a complex with formula $TlCl_4^{=}$ (dissociation constant, 93; absorption maximum, 254 mμ) exists.

2. The solubility data of TlI in KI solutions due to Kul'ba were analyzed by the method of Scott and Hu. The following complexes and dissociation constants were consistent with the data: TlI, 0.034; TlI_2^-, 0.26; $TlI_3^=$, 2.0; $TlI_4^{\equiv}$, 3.5.

3. The fluorescence emission spectra of KCl:TlCl solutions were analyzed with the assistance of the dissociation constants of the complex species. The broad fluorescence band with maximum at 440 mμ was found to be due to the overlap of four symmetric bands, of which the maximum is at 370, 435-440, and 450 mμ for Tl^+, TlCl and $TlCl_2^-$, and $TlCl_4^{=}$ respectively. The order of the fluorescence quantum yields is $TlCl_4^{=} > TlCl_2^- \cong TlCl > Tl^+$.

4. Analysis of the fluorescence emission spectrum of KBr:TlBr solutions showed that the broad fluorescence band with maximum at 480 mμ is due to the overlap of three symmetric bands with the maximum at 440 mμ for TlBr, 475 mμ for $TlBr_2^-$, and 495 mμ for $TlBr_4^{=}$. The order of the fluorescence quantum yields is $TlBr > TlBr_2^- > TlBr_4^{=}$.

5. The thallous iodide complexes, in contrast to the strong fluorescence of thallous chloride and bromide complexes, exhibit very weak fluorescence. The maximum intensity of the fluorescence

band is at 500-520 mμ. The low fluorescence yield may be due to dissipation of the energy by photochemical reactions or quenching by iodide ions.

6. Approximate metal-ligand bond energies were calculated with the assistance of experimental dissociation constants, hydration enthalpies, and entropies. Metal-ligand bond energies were calculated to be -9.5, -10.6, -11.4, and -13.7 kcal/mole for Tl-H_2O, Tl-Cl, Tl-Br, and Tl-I respectively.

7. The absorption spectrum of thallous chloride and thallous bromide complexes was considered from the standpoint of electron transfer transitions. The absorption maximum of these transitions is shifted toward longer wavelengths as the reducing strength of the halide ligand increases and as the number of coordinated ligands increases. It is proposed that the electron transfer is from a halide ligand to the thallous ion. The oscillator strengths of the transitions are approximately 0.1.

8. The similarity of the absorption and emission spectra of thallium-containing potassium halide single crystal phosphors with that of the thallous halide complexes is demonstrated; the conclusion is made that the spectra of the single crystal phosphors may be attributed to complex aggregates in the crystal lattice and that treatment of the spectra from the standpoint of electron transfer would be worthwhile.

SUGGESTIONS FOR FURTHER STUDY

The following are suggestions for further experimental work:

a) radioactive tracer studies to determine the lability of thallous halide complexes.

b) absorption measurements on KI:TlI solutions under conditions which avoid interference from I_3^- so that molar absorptivities could be assigned to the thallous iodide complexes.

c) fluorescence polarization and nuclear magnetic moments measurement to aid in the elucidation of the structure of the complexes.

d) absorption and emission studies on single crystals of KNO_3:Tl (or other substances which do not complex with thallium) to test the validy or lack of validity of the Seitz-Williams model of the luminescence center.

e) the use of non-aqueous solvents in order to assess the role of the solvent in the fluorescence of the complexes.

BIBLIOGRAPHY

1. Alentsev, M.N. and L.O. Pakhomycheva. Concerning the relation between the absorption and luminescence spectra of complex molecules. Bulletin of the Academy of Sciences of the USSR, Physical Series 24:737-739. 1960.

2. Avramenko, V.G. and M.U. Belyi. Absorption and luminescence centers in thallium solutions. Bulletin of the Academy of Sciences of the USSR, Physical Series 23:67-70. 1959.

3. Balchan, A.S. and H.G. Drickamer. Effect of pressure and temperature on the absorption spectra of four alkali halide phosphors. The Journal of Chemical Physics 35:359-361. 1961.

4. Barrow, G.M. Introduction to molecular spectroscopy. New York, McGraw-Hill, 1962. 318p.

5. Basolo, F. and R.G. Pearson. Mechanisms of inorganic reactions. New York, Wiley, 1958. 426p.

6. Belyi, M.U. and B.F. Rud'ko. Influence of temperature on the luminescence of halide solutions of heavy metals. Bulletin of the Academy of Sciences of the USSR, Physical Series 24: 588-592. 1960.

7. Brauer, P. and D. Pelte. Über die Lumineszenzspektren wässriger Thalliumsalzlösungen ohne und mit Zusatz von Alkalihalogenid. Zeitschrift für Naturforschung 17A:875-883. 1962.

8. Buenger, W. Messung der Lichtemission von Alkalihalogenidphosphoren. Zeitschrift für Physik 66:311-327. 1930.

9. Buenger, W. and W. Flechsig. Über die Abklingung eines KCl-Phosphors mit TlCl-Zusatz und ihre Temperaturabhängigkeit. Zeitschrift für Physik 67:42-53. 1931.

10. Buenger, W. and W. Flechsig. Über die Auslöschungsverteilung von einigen Alkalihalogenidphosphoren und die Quantenausbeute der Ausleuchtung an einem KCl-Phosphor mit Tl-Zusatz. Zeitschrift für Physik 69:637-653. 1931.

11. Day, M.C. and J. Selbin. Theoretical inorganic chemistry. New York, Reinhold, 1962. 413p.

12. Dexter, D.L. and J.H. Schulman. Theory of concentration quenching in inorganic phosphors. The Journal of Chemical Physics 22:1063-1070. 1954.

13. Dunn, T.M. The visible and ultra-violet spectra of complex compounds. In: Modern coordination chemistry, ed. by J. Lewis and R.G. Wilkins. New York, Interscience, 1960. p. 229-300.

14. Forsythe, W.E. (ed.). Measurement of radiant energy. New York, McGraw-Hill, 1937. 452p.

15. Fromherz, Hans. Optische Beziehung zwischen Alkalihalogenid-phorphoren und Komplexsalzlösungen von Blei- und Thallo-halogeniden. Zeitschrift für Physik 68:233-243. 1931.

16. Fromherz, H. and W. Menschick. Optische Beziehungen zwischen Alkalihalogenidphosphoren und Komplexsalzlösungen. Zeitschrift für Physikalische Chemie, Abt. B, 3:1-40. 1929.

17. Garlick, G.F.J. Luminescence. In: Handbuch der Physik, ed. by S. Flügge. vol. 26. Berlin, Springer Verlag, 1958. p. 1-128.

18. Gillespie, L.J. ed. Density (specific gravity) and thermal expansion (under atmospheric pressure) of aqueous solutions of inorganic substances and of strong electrolytes. In: International Critical Tables, vol. 3. New York, McGraw-Hill, 1928. p. 51-111.

19. Hardtke, F.C. Photoconduction fatigue in colored potassium chloride. Ph.D. thesis. Corvallis, Oregon State University, 1959. 117 numb. leaves.

20. Harned, H.S. The electromotive forces of uni-univalent halides in concentrated aqueous solutions. Journal of the American Chemical Society 51:416-427. 1925.

21. Hatchard, C.G. and C.A. Parker. A new sensitive chemical actinometer. II Potassium ferrioxalate as a standard chemical actinometer. Proceedings of the Royal Society (London) 235A:518-536. 1956.

22. Hersh, H.N. Spectra of halogen solutions and V-bands in alkali halides. Physical Review 105:1410-1411. 1957.

23. Hilsch, R. Alkali-halide phosphors containing heavy metals. Proceedings of the Physical Society (London) 49 Extra part: 40-45. 1937.

24. Hu, Kuo-Hao and Allen B. Scott. Thallous complexes in chloride solutions. Journal of the American Chemical Society 77: 1380-1382. 1955.

25. Ivanova, N.I., L.I. Tarasova and A.P. Zhukouski. Origin of the long wavelength luminescence bands of alkali-halide phosphors. Bulletin of the Academy of Sciences of the USSR, Physical Series 25:331-333. 1961.

26. Johnson, P.D. Configuration coordinate model for luminescence in KCl:Tl. The Journal of Chemical Physics 22:1143. 1954.

27. Johnson, P.D. and F.E. Williams. Energy levels and rate processes in the thallium-activated potassium chloride phosphor. The Journal of Chemical Physics 20:124-128. 1952.

28. Johnson, P.D. and F.E. Williams. Electron traps in the thallium-activated potassium chloride phosphor. The Journal of Chemical Physics 21:125-130. 1953.

29. Johnson, P.D. and F.E. Williams. Simplified configuration coordinate model for KCl:Tl. Physical Review 117:964-969. 1960.

30. Jørgensen, C.K. Absorption spectra and chemical bonding in complexes. London, Pergamon Press, 1962. 352p.

31. Joshi, R.V. Temperature dependence of the ultraviolet and visible phosphorescence in KCl:Tl. Physica 27:1119-1128. 1961.

32. Katzin, L.I. Regularities in the absorption spectra of halides. The Journal of Chemical Physics 23:2055-2060. 1955.

33. Kauzmann, W. Quantum chemistry. New York, Academic Press, 1957. 744p.

34. Ketelaar, J.A.A. Chemical constitution. 2d rev. ed. Amsterdam, Elsevier, 1958. 448p.

35. Kortüm, G. and J. Bockris. Textbook of electrochemistry. Vol. 1. New York, Elsevier, 1951. 351p.

36. Kul'ba, F. Ya and V.E. Mironov. Formation of complex iodides of monovalent thallium in solution. I., II. Russian Journal of Inorganic Chemistry vol. 2 pt. 6:78-96. 1957.

37. Kul'ba, F. Ya and V.E. Mironov. Formation of complex iodides of monovalent thallium in solution. III. Russian Journal of Inorganic Chemistry vol. 3 pt. 6:68-76. 1958.

38. Kul'ba, F. Ya, V.E. Mironov and V.A. Federov. Complexes of thallium (I) with alkali metal halides. Russian Journal of Inorganic Chemistry 6:813-816. 1961.

39. Makishima, S., T. Tomotsu, M. Hirata, R. Kambe and S. Shinoya. Polarization of low temperature luminescence from thallium-containing sodium nitrite single crystals. Physics and Chemistry of Solids 18:262-264. 1961.

40. McConnell, H., J.S. Ham and J.R. Platt. Regularities in the spectra of molecular complexes. The Journal of Chemical Physics 21:66-70. 1953.

41. Merritt, C., H.M. Hershenson and L.B. Rogers. Spectrophotometric determination of bismuth, lead, and thallium with hydrochloric acid. Analytical Chemistry 25:572-577. 1953.

42. Morgenshtern, Z.L. Measurement of the absolute quantum yield of photoluminescence of alkali-halide crystals. Soviet Physics, JETP 2:73-74. 1956.

43. Nancollas, G.H. Thermodynamics of ion association. Discussions of the Faraday Society 24:108-113. 1957.

44. Nilsson, R.O. The complex formation between thallium (I) ions and halide, thiocyanate, and cyanide ions. Arkiv för kemi 10:363-381. 1957.

45. Parker, C.A. and W.T. Reis. Correction of fluorescence spectra and measurement of fluorescence quantum efficiency. Analyst 85:587-600. 1960.

46. Pauling, Linus. The nature of the chemical bond. 3d ed. Ithaca, Cornell University Press, 1960. 644p.

47. Pringsheim, Peter. Fluorescence and phosphorescence. New York, Interscience Publishers, 1949. 794p.

48. Pringsheim, Peter. Fluorescence and phosphorescence of thallium-activated potassium halide phosphors. Reviews of Modern Physics 14:132-138. 1942.

49. Pringsheim, Peter and H. Vogels. Fluoreszenz von Schwermetallkomplexen in Wässerigen Lösung. Physica 7:225-240. 1940.

50. Radio Corporation of America. RCA photosensitive devices and cathode-ray tubes. Harrison, N.J., 1960. 35p.

51. Rebane, L.A. Concentration and temperature quenching of luminescence in some silver activated alkali-halide phosphors. Bulletin of the Academy of Sciences of the USSR, Physical Series 25:335-337. 1961.

52. Rossini, F.D. et al. Selected values of chemical thermodynamic properties. National Bureau of Standards Circular 500. Washington, United States Government Printing Office, 1952. 1268p.

53. Rossotti, F.J.C. The thermodynamics of metal ion complex formation in solution. In: Modern coordination chemistry. ed. by J. Lewis and R.G. Wilkins. New York, Interscience, 1960. p. 1-77.

54. Saur, E. and O. Stasiw. Einfluss geringer Fremdionenzusätze auf die Gitterkonstante von Alkalihalogenidkristallen. Nachrichten von der Gesellschaft der Wissenschaft zu Göttingen, Mathematische-Physikalische Classe, Neue Folge, Fachgruppe II 3:77-83. 1938.

55. Scott, Allen B. and Kuo-Hao Hu. Absorption spectra of luminescent thallous chloride solutions. The Journal of Chemical Physics 23:1830-1833. 1955.

56. Scott, Allen B., R.G. Dartau and Surang Sapsoonthorn. Bromide complexes of thallium (I). Inorganic Chemistry 1:313-316. 1962.

57. Seitz, F. Interpretation of the properties of alkali halide-thallium phosphors. The Journal of Chemical Physics 6:150-162. 1938.

58. Shinoya, S. The Institute for Solid State Physics. The University of Tokyo, Japan. Luminescence of thallous complex ions. (Personal Communication)

59. Sienko, M.J. and R.A. Plane. Physical inorganic chemistry. New York, W.A. Benjamin, 1963. 166p.

60. Sill, C.W. and H.E. Peterson. Fluorescence test for thallium in aqueous solution. Analytical Chemistry 21:1266-1268. 1949.

61. Stepanov, B.I. and A.M. Samson. The theory of the absorption and luminescence of complex molecules. Optics and Spectroscopy 12:224-232. 1962.

62. Udenfreund, Sidney. Fluorescence assay in biology and medicine. New York, Academic Press, 1962. 505p.

63. Vitol, I.K. and I.K. Plyavin. The kinetics of the short-lived photoluminescence of some activated alkali halide crystals. Optics and Spectroscopy 9:189-191. 1960.

64. Weinreb, A. Some effects of temperature and viscosity on fluorescence and energy transfer in solutions. The Journal of Chemical Physics 35:91-102. 1961.

65. White, C.E., May Ho and E.Q. Weimer. Methods for obtaining correction factors for fluorescence spectra as determined with the Aminco-Bowman spectrophotofluorometer. Analytical Chemistry 32:438-440. 1960.

66. Williams, F.E. An absolute theory of solid-state luminescence. The Journal of Chemical Physics 19:457-466. 1951.

67. Williams, F.E. The luminescence of inorganic crystals. Journal of Chemical Education 38:242-250. 1961.

68. Williams, F.E., B. Segall and P.D. Johnson. Oscillator strengths for luminescent transitions in KCl:Tl and KCl:In. Physical Review 108:46-49. 1957.

69. Yuster, P.H. and C.J. Delbecq. Some optical properties of potassium iodide-thallium phosphors. The Journal of Chemical Physics 21:892-898. 1953.